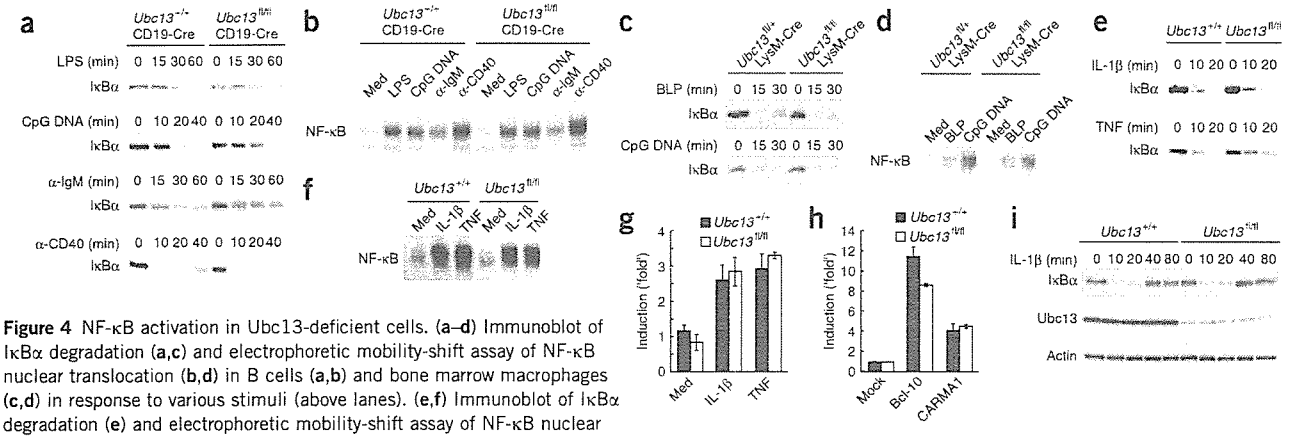

Figure 4 NF-κB activation in Ubc13-deficient cells. (**a–d**) Immunoblot of IκBα degradation (**a**,**c**) and electrophoretic mobility-shift assay of NF-κB nuclear translocation (**b**,**d**) in B cells (**a**,**b**) and bone marrow macrophages (**c**,**d**) in response to various stimuli (above lanes). (**e**,**f**) Immunoblot of IκBα degradation (**e**) and electrophoretic mobility-shift assay of NF-κB nuclear translocation (**f**) in MEFs in response to various stimuli (above lanes). (**g**) NF-κB luciferase reporter activity in whole-cell lysates of MEFs stimulated with 10 ng/ml of IL-1β or 10 ng/ml of TNF. (**h**) NF-κB luciferase reporter activity in whole-cell lysates of MEFs transfected with plasmids encoding Bcl-10 or CARMA1. (**i**) Immunoblot of IκBα degradation and recovery in MEFs stimulated with 10 ng/ml of IL-1β (time, above lanes). Data are representative of two (**i**) or three (**a–h**) independent experiments.

These data indicate that Ubc13 is critically involved in MAP kinase activation, yet has only a minor function in NF-κB activation. To elucidate precisely where in the TLR, IL-1R, BCR and CD40 signaling pathways Ubc13 induces MAP kinase activation, we examined the activation and modification of signaling molecules 'upstream' of the IKK complex and MAP kinase kinase proteins. *In vitro* studies indicate that IL-1β stimulates TRAF6 ubiquitination in a Ubc13-dependent way[16]. Therefore, we examined IL-1β-induced polyubiquitination of TRAF6 in control or *Ubc13*$^{fl/fl}$ MEFs expressing retroviral Cre. IL-1β-induced polyubiquitination of TRAF6 was evident in control and *Ubc13*$^{fl/fl}$ MEFs expressing retroviral Cre (**Fig. 6a**). As the K63-linked ubiquitination of TRAF6 has been linked to activation of the kinase TAK1 (ref. 17), we next examined IL-1β-mediated TAK1 phosphorylation in control and *Ubc13*$^{fl/fl}$ MEFs expressing retroviral Cre. These MEFs had similar amounts of phosphorylated TAK1, albeit with delayed kinetics in *Ubc13*$^{fl/fl}$ MEFs compared with control MEFs (**Fig. 6b**). Next we undertook a biochemical approach in which we added recombinant TRAF6 to extracts from unstimulated control cells, which results in phosphorylation of TAK1 and IKK proteins[16,17] (**Fig. 6c**). The addition of TRAF6 to extracts of *Ubc13*$^{fl/fl}$ MEFs expressing retroviral Cre resulted in slightly impaired TAK1 phosphorylation and normal phosphorylation of IKK proteins. These results suggested that Ubc13 is involved in TAK1 activation but that Ubc13 is not absolutely essential for IL-1β-induced TAK1 activation.

Given that TAK1 is critical in IL-1β-induced activation of NF-κB and MAP kinases[18,19] and that there was considerable activation of TAK1 and NF-κB in *Ubc13*$^{fl/fl}$ MEFs expressing retroviral Cre, TAK1 activation might contribute to the substantial IL-1β-induced NF-κB

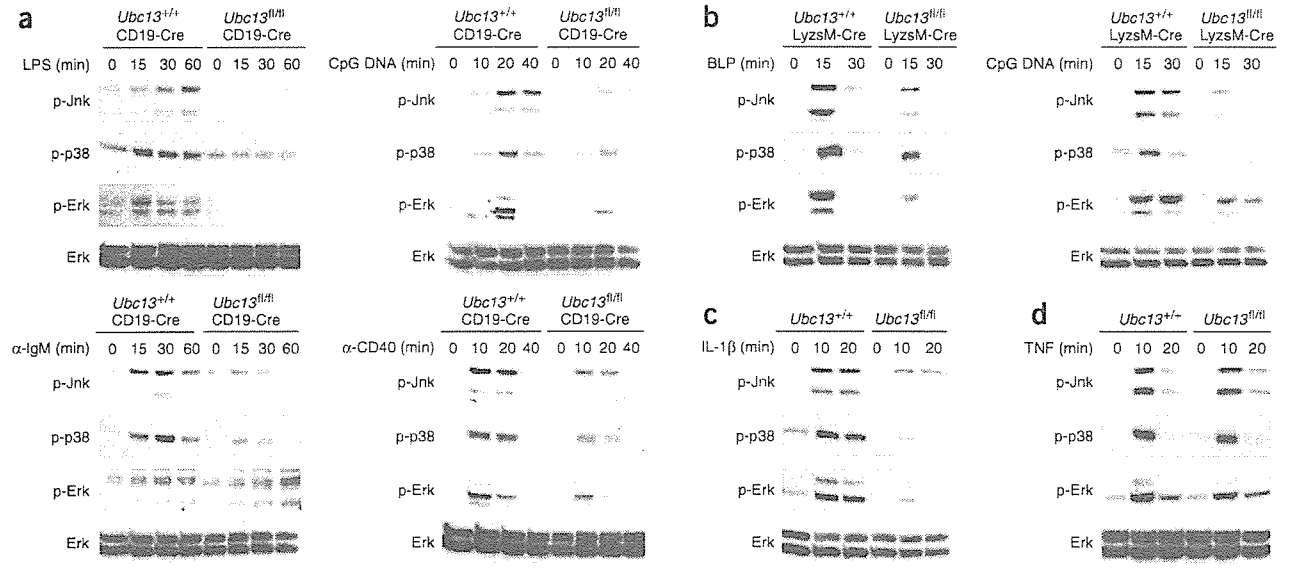

Figure 5 Impaired MAP kinase activation in Ubc13-deficient cells. (**a**) Immunoblot of whole-cell lysates of B cells stimulated with 10 μg/ml of LPS, 1 μM CpG DNA, 10 μg/ml of anti-IgM or 10 μg/ml of anti-CD40. (**b**) Immunoblot of whole-cell lysates of bone marrow macrophages stimulated with 100 ng/ml of BLP or 1 μM CpG DNA. (**c**,**d**) Immunoblot of whole-cell lysates of MEFs stimulated with 10 ng/ml of IL-1β (**c**) or 10 ng/ml of TNF (**d**). p-, phosphorylated. Data are representative of three independent experiments.

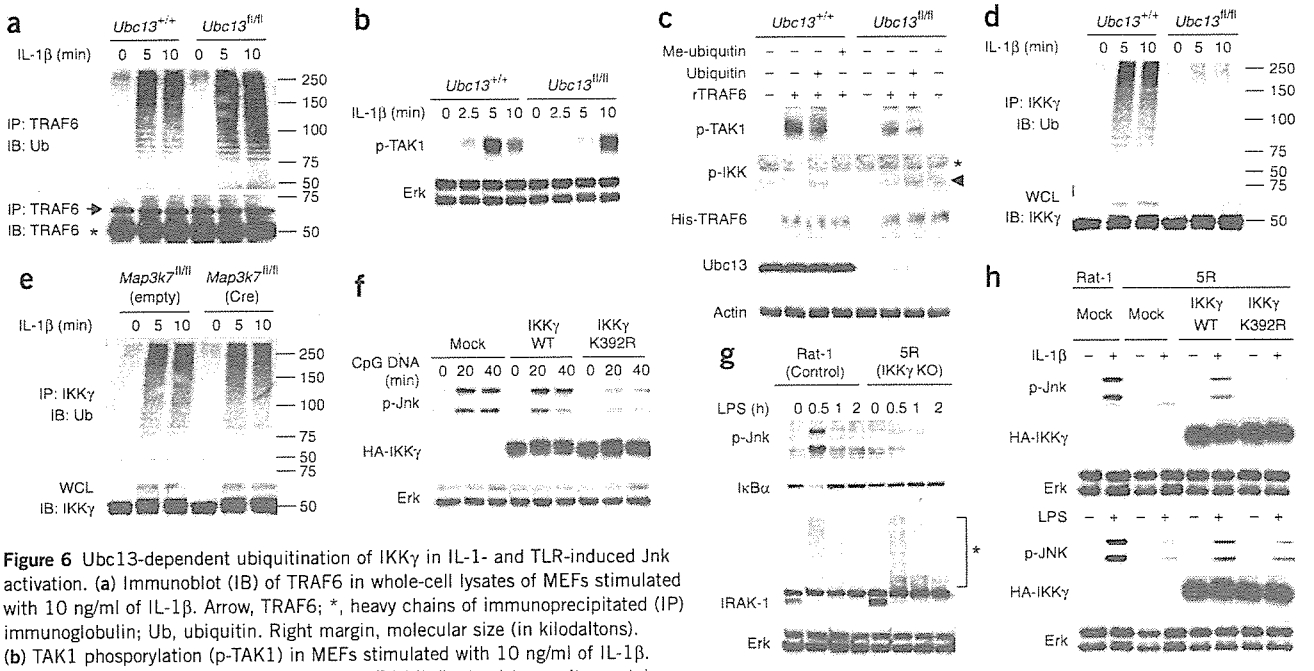

Figure 6 Ubc13-dependent ubiquitination of IKKγ in IL-1- and TLR-induced Jnk activation. (**a**) Immunoblot (IB) of TRAF6 in whole-cell lysates of MEFs stimulated with 10 ng/ml of IL-1β. Arrow, TRAF6; *, heavy chains of immunoprecipitated (IP) immunoglobulin; Ub, ubiquitin. Right margin, molecular size (in kilodaltons). (**b**) TAK1 phosporylation (p-TAK1) in MEFs stimulated with 10 ng/ml of IL-1β. The same lysates were also blotted with anti-Erk1/2 (bottom) to monitor protein expression. (**c**) Immunoblot of cell extracts of MEFs incubated with recombinant TRAF6 (rTRAF6) in the presence of ubiquitin or methylated ubiquitin (Me-ubiquitin). Arrowhead, phosphorylated IKK (p-IKK); *, nonspecific bands; His-, histidine-tagged. (**d**) Immunoblot of IKKγ immunoprecipitates from whole-cell lysates of MEFs stimulated with 10 ng/ml of IL-1β. (**e**) Immunoblot of IKKγ immunoprecipitates from whole-cell lysates of MEFs stimulated with 10 ng/ml of IL-1β. *Map3k7*$^{fl/fl}$, *loxP*-flanked gene encoding TAK1, with (Cre) and without (empty) Cre recombinase. WCL (bottom, **d**,**e**), immunoblot of whole-cell lysates without immunoprecipitation. (**f**) Immunoblot of whole-cell lysates from 70Z/3 pre–B cell lines stably transfected with wild-type (WT) or K392R IKKγ expression vectors. HA-, hemagglutinin-tagged. (**g**) Immunoblot of whole-cell lysates of Rat-1 or 5R cells stimulated with 10 μg/ml of LPS. *, ubiquitinated IRAK-1. (**h**) Immunoblot of whole-cell lysates of Rat-1 or 5R cells stably expressing wild-type or K392R IKKγ expression vectors, stimulated with 10 ng/ml of IL-1β (top) or 10 μg/ml of LPS (bottom). Data are representative of two (**a**,**b**,**d**,**f**,**g**,**h**) or three (**c**,**e**) independent experiments.

activation in the absence of Ubc13. However, given the impaired IL-1β-induced MAP kinase activation in Ubc13-deficient cells, full activation of TAK1 alone may be insufficient for full activation of MAP kinases. Ubc13 has also been suggested to be involved in TCR-induced ubiquitination of IKKγ[15]. We found that IL-1β also stimulated IKKγ polyubiquitination in control MEFs, but that IL-1β-induced IKKγ polyubiquitination was impaired in *Ubc13*$^{fl/fl}$ MEFs expressing retroviral Cre (**Fig. 6d**). Moreover, IL-1β-induced polyubiquitination of IKKγ was normal in TAK1-deficient MEFs (**Fig. 6e**), suggesting that the Ubc13-dependent ubiquitination of IKKγ is a TAK1-independent signaling event.

These aforementioned results prompted us to examine whether the ubiquitination of IKKγ is involved in TLR- and IL-1R-induced MAP kinase activation. As lysine 392 (K392) of mouse IKKγ is known to be the acceptor lysine residue for Ubc13-dependent polyubiquitination[24], we generated a K392R mouse IKKγ mutant and compared CpG DNA–induced Jnk activation in the mouse pre–B cell line 70Z/3 expressing wild-type or K392R IKKγ constructs. The 70Z/3 cells expressing K392R IKKγ had defective activation of Jnk in response to CpG DNA relative to that of mock-transfected 70Z/3 cells or 70Z/3 cells expressing wild-type IKKγ, suggesting that IKKγ K392R inhibits CpG DNA–mediated Jnk activation in a dominant negative way (**Fig. 6f**). Moreover, activation of Jnk and p38 induced by CpG DNA or by phorbol 12-myristate 13-acetate plus ionomycin was impaired in IKKγ-deficient 1.3E2 cells relative to that in control 70Z/3 cells (**Supplementary Fig. 4** online). We further investigated stimulus-dependent activation of MAP kinases in other cell types. MAP kinase activation in response to LPS or IL-1β was reduced considerably in the rat IKKγ-deficient fibroblast cell line 5R as well as in IKKγ-deficient MEFs (**Fig. 6g** and **Supplementary Fig. 4**), indicating that IKKγ is essential for full activation of MAP kinases in response to multiple immune stimuli. To clarify whether ubiquitination of IKKγ is necessary for full MAP kinase activation, we retrovirally expressed wild-type or K392R IKKγ in the IKKγ-deficient 5R fibroblasts and analyzed IL-1β- and LPS-induced Jnk activation. Ectopic expression of wild-type IKKγ induced considerable Jnk activation (**Fig. 6h**). In contrast, K392R IKKγ permitted much weaker Jnk activation. These results indicate that Ubc13-dependent IKKγ ubiquitination may have a partial function in IL-1R- and TLR-induced MAP kinase activation.

DISCUSSION

Here we used a conditional ablation strategy to analyze the physiological function of Ubc13. Ubc13-deficient cells showed almost normal NF-κB activation and severely impaired MAP kinase activation in response to a variety of stimuli, except for TNF. *Ubc13* disruption in bone marrow macrophages resulted in impaired TLR-induced proinflammatory cytokine production and MAP kinase activation. Macrophages treated with MAP kinase inhibitors show defective cytokine production[34,35] and cells lacking MAP kinase phosphatase 5, which show augmented stimulus-dependent Jnk activation, conversely produce increased amounts of cytokines[36], suggesting that MAP kinase activation promotes TLR-induced cytokine production. Failure to activate MAP kinases after TLR stimulation

may have contributed to the reduced cytokine production in Ubc13-deficient bone marrow macrophages. However, there was normal TLR-mediated MyD88-independent expression of type I interferon and interferon-inducible genes in Ubc13-deficient cells, suggesting that Ubc13 is dispensable for TLR-mediated MyD88-independent immune responses.

Ubc13-deficient B cells showed impaired BCR-, CD40- and TLR-mediated activation. In terms of B cell development, mice lacking components of the BCR signaling pathway have phenotypes similar to that of *Ubc13*$^{fl/fl}$Cd19-Cre mice. For example, development of marginal zone B cells and B-1 cells is compromised in *Bcl10*$^{-/-}$ mice and *Malt1*$^{-/-}$ mice[9,13,31]. Although investigation of marginal zone B cells in CARMA1-deficient (*Card11*$^{-/-}$) mice has not been reported, these mice have substantially impaired development of B-1 cells[10–12,14]. Moreover B-1 cell populations are considerably reduced in the peritoneal cavities of mice lacking TAK1, which also participates in BCR signaling[19,37]. Thus, these similarities indicate that Ubc13 may be involved in BCR signaling pathways that are essential for the development of certain B cell lineages. Contrary to published results showing that Ubc13 is involved in TNFR- and TRAF2-dependent activation of NF-κB or MAP kinases[16,28,38], Ubc13-deficient MEFs showed normal TNF-induced activation of NF-κB and MAP kinases, indicating that Ubc13 might have a minor function in TNFR-mediated activation in this cell type.

In response to IL-1β and TLR ligands, Ubc13-deficient cells showed almost normal NF-κB activation and considerable impairment in MAP kinase activation. In addition, there was unexpected IL-1β-induced polyubiquitination of TRAF6 in Ubc13-deficient MEFs. *In vitro* ubiquitination assays in which only Ubc13 and Uev1A E2 ubiquitin ligases are present have shown that TRAF2 and TRAF6 are involved in the generation of K63-linked but not K48-linked polyubiquitin chains[15,16]. However, given that overexpression of TRAF2 *in vivo* generates K63- as well as K48-linked ubiquitination[28], IL-1β-induced Ubc13-independent K48-linked but not Ubc13-dependent K63-linked ubiquitination of TRAF6 might be detected in Ubc13-deficient MEFs. Alternatively, another E2 conjugating enzyme, UbcH7, has been shown to facilitate TRAF6-related K63-linked polyubiquitination[39]. UbcH7 might compensate for the lack of Ubc13 and stimulate IL-1β-induced K63-linked ubiquitination of TRAF6.

Ubc13-dependent ubiquitination is involved in TAK1 activation[17]. Here, Ubc13-deficient MEFs showed almost normal TAK1 phosphorylation, albeit with substantially delayed kinetics, suggesting that Ubc13 is not absolutely required for full activation of TAK1. Analysis of TAK1-deficient cells has demonstrated that TAK1 is essential in TLR- and IL-1R-induced activation of NF-κB and MAP kinases[18,19]. Therefore, we propose that although full TAK1 activation alone may be sufficient to induce considerable NF-κB activation in response to IL-1β, supplemental signaling events 'downstream' of or independent of TAK1 might also be required for the efficient activation of MAP kinases.

Several *in vitro* experiments have demonstrated that IKKγ is ubiquitinated in a Ubc13-dependent way[15,24,27]. In our study here, IL-1β-mediated ubiquitination of IKKγ was considerably impaired in Ubc13-deficient MEFs but was normal in TAK1-deficient cells, suggesting possible involvement of IKKγ ubiquitination in MAP kinase activation. Overexpression of the ubiquitination-deficient K392R IKKγ mutant reduced Jnk activation in 70Z/3 cells. In addition, the derivative IKKγ-deficient cell line 1.3E2 showed defective Jnk and p38 activation in response to CpG DNA (or phorbol 12-myristate 13-acetate plus ionomycin). Indeed, characterization of IKKγ-deficient 1.3E2 cells has demonstrated 'normal' MAP kinase activation in response to stimulation with phorbol 12-myristate 13-acetate plus ionomycin[40]. In contrast, another study has shown that although 1.3E2 cells have impaired Jnk activation in response to the same stimuli tested in that previous study[40], responsiveness is restored by ectopic expression of protein kinase C-θ (PKC-θ), PKC-δ or IKKγ; that study concluded that 1.3E2 cells lack PKC-θ and PKC-δ in addition to PKC-θ and PKC-δ[41]. However, as we reproducibly found impairment in the activation of Jnk and p38 in several IKKγ-deficient cell lines, we believe that IKKγ might be involved in the stimulus-dependent activation of the MAP kinases as well as NF-κB in these cell types. Furthermore, re-expression of the K392R IKKγ mutant, to which K63-linked polyubiquitin chains cannot be appended, in IKKγ-deficient 5R cells conferred much weaker Jnk activation in response to IL-1β and LPS than did wild-type IKKγ, suggesting that Ubc13-dependent IKKγ ubiquitination may be essential at least in part for Jnk activation. The IKKγ-interacting protein Act1 (also called CIKS), whose overexpression potentiates Jnk and NF-κB activation, might be involved in IKKγ-related Jnk activation[42,43]. Studies using Act1-deficient cells may allow examination of that possibility[44].

Although IKKγ deficiency resulted in defective activation of MAP kinases in our study, IKKγ-deficient cell lines may have mutated in the interim between previously published studies and our studies here, resulting in loss of the original phenotype of 'normal' MAP kinase activation reported before[40]. Further analysis using 'knock-in' mice homozygous for the mutation producing the IKKγ K392R substitution will provide physiological conditions in which to examine whether Ubc13-dependent ubiqituitination of IKKγ is involved in the activation of MAP kinases (as well as NF-κB) in response to various stimuli in other cell types and immune responses.

As for the involvement of Ubc13 in NF-κB activation, given that mice lacking either IKKβ or IKKγ, both of which are essential for BCR-induced NF-κB activation, also show defects in the development of marginal zone B cells and B-1 cells[45,46], Ubc13 might be critical to IKKβ-dependent NF-κB activation in a cell type–specific way. Moreover, we cannot exclude the possibility that conditional deletion of Ubc13 may have been incomplete in some cell types or that another E2 family member (such as Ubc5, which is involved in IκBα phosphorylation[47] and K63-linked polyubiquitin chain synthesis[48]) compensated for the loss of Ubc13 in some cell types. Further studies are needed to comprehensively evaluate the function of Ubc13 in NF-κB activation using other cell types such as T cells, hepatocytes and keratinocytes.

In summary, here we have provided genetic evidence that Ubc13 is involved in TLR-, IL-1R-, BCR- and CD40-mediated immune responses in several cell types. We have demonstrated that Ubc13 deficiency 'preferentially' affects the activation of MAP kinases at least in part through induction of ubiquitination of IKKγ. Further studies using conditionally Ubc13-deficient mice may provide a new insight into other Ubc13-dependent, K63-linked, ubiquitination-related biological processes, such as those induced by DNA repair and cellular stress.

METHODS

Generation of *Ubc13*$^{fl/fl}$ mice. Genomic DNA containing *Ubc13* was isolated from a 129/Sv mouse genomic library and was characterized by restriction enzyme mapping and sequencing analysis. The targeting vector was constructed by replacement of a 3.0-kilobase fragment of *Ubc13* with a neomycin-resistance gene cassette. In addition, a 3.0-kilobase fragment of *Ubc13* genomic DNA containing exons 2, 3 and 4 was inserted between two *lox*P sites in the targeting vector pKSTKNEOLOXP, which contains a herpes simplex virus thymidine kinase gene driven by a PGK promoter. The targeting vector was transfected into embryonic stem cells (embryonic day 14.1). Colonies resistant to both G418 and ganciclovir were screened. Homologous recombinants were microinjected into C57BL/6 female mice, and heterozygous F_1 progeny were

intercrossed to generate *Ubc13*$^{fl/fl}$ mice. All animal experiments were done with the approval of the Animal Research Committee of the Research Institute for Microbial Diseases of Osaka University (Osaka, Japan).

Reagents, cells and mice. LPS, poly(I:C), BLP, MALP-2 and CpG oligodeoxynucleotides were prepared as described[42]. Agonistic anti-CD40 and anti-IgM were purchased from PharMingen. B cell–activating factor of the TNF family, IL-1β and TNF were from Genzyme. Antibodies specific for the phosphorylated forms of Erk (9101), Jnk (9251), p38 (9211), IKK (3031) and IκBα (9241) were purchased from Cell Signaling. Antibodies specific for Erk (sc-94), IκBα (sc-371), TRAF6 (sc-7221), IKKγ (sc-8330), ubiquitin (sc-8017), hemagglutinin (sc-3792), histidine (sc-8036), actin (sc-8432) and NF-κBp52 (sc-298) were from Santa Cruz. Monoclonal anti-Ubc13 (37-1100) was from Zymed. Anti-IRAK-1 and anti-phospho-TAK1 have been described[49,50]. The IKKγ-deficient cell line 5R and control cell line Rat-1 (ref. 51), the IKKγ-deficient cell line 1.3E2 and control cell line 70Z/3 (ref. 40), IKK-γ-deficient MEFs[52] and MEFs homozygous for *lox*P-flanked TAK1 and expressing retroviral Cre[19] have been described. Cd19-Cre and LyzsM-Cre mice have been described[53,54].

Preparation of bone marrow macrophages. Bone marrow cells were isolated from femurs and were cultured in RPMI 1640 medium supplemented with 10% FBS and 50 ng/ml of macrophage colony-stimulating factor (R&D Systems). Medium was replaced every 2.5 d. In these conditions, monolayers of adherent cells of which more than 99% expressed surface Mac-1 were obtained. Cells were collected by incubation with 10 mM EDTA in PBS with gentle agitation and were seeded onto plates. After culture for several hours without macrophage colony-stimulating factor, cells were used as bone marrow macrophages.

Measurement of proinflammatory cytokines and electrophoretic mobility-shift assay. These assays were done as described[55].

Purification of B cells and splenic CD4$^+$ T cells. Resting B cells were isolated from splenocyte single-cell suspensions by positive selection with anti-B220 magnetic beads (Miltenyi Biotec). Cell purity was typically more than 97% for B220$^+$ cells, as assessed by flow cytometry.

Plasmids and retroviral transduction. The NF-κB-dependent reporter plasmids and expression vectors containing *Card11* have been described[55,56]. The retroviral vector pMRX encoding Cre protein and the production of retroviruses have been described[19]. At 12 h after infection, 3 μg/ml of puromycin (Invivogen) was added and selected cells were analyzed 48–72 h after infection. Hemagglutinin-tagged wild-type and K392R IKKγ constructs were generated by PCR and were cloned into pMRX retroviral vectors as described[57].

Luciferase reporter assay. This reporter assay was done with the Dual-Luciferase Reporter Assay System (Promega) as described[57].

Immunoblot, immunoprecipitation and *in vivo* ubiquitination assay. After several hours of 'starvation' in DMEM containing 0.1% FBS (to reduce background signal), cells were stimulated with various ligands for various times. Immunoblot and immunoprecipitation were done as described[57]. For detection of *in vivo* ubiquitination of IKKγ and TRAF6, cell lysates were boiled for 10 min at 90 °C in 1% SDS for removal of noncovalently attached proteins, followed by immunoprecipitation with anti-IKKγ or anti-TRAF6 in 0.1% SDS lysis buffer in the presence of protease inhibitors. Ubiquitin was detected by immunoblot anlaysis.

Cell viability assay. Purified splenic B cells (1×10^6) were stimulated with various ligands for various times. Cell viability was assessed with the MEBCYTO Apoptosis kit (MBL) and a FACSCalibur (Becton Dickinson).

Lymphocyte proliferation assay, cell cycle analysis and flow cytometry. These assays were done as described[19].

***In vivo* immunization and enzyme-linked immunosorbent assay (ELISA).** These assays were done as described[19].

Immunohistochemistry. Spleen tissue was embedded in optimum cutting temperature compound (Lab-Tek Products) and was 'flash frozen' in liquid nitrogen. Sections 5 μm in thickness were fixed in cold acetone, were air-dried and were incubated for 1 h at 25 °C in PBS containing 1% BSA, 10% normal rat serum and 5% normal goat serum. Tissue sections were then stained for 60 min at 25 °C with biotin-conjugated anti-mouse CD19 (Pharmingen) followed by streptavidin-conjugated alkaline phosphatase for 30 min, or with rat monoclonal antibody to mouse metallophilic macrophages (MCA947F; Serotec) followed by horseradish peroxidase–conjugated anti-rat. After being stained, sections were washed and were developed with the Vector Blue Alkaline Phosphatase Substrate Kit or the AEC (3-amino-9-ethylcarbazole) Substrate Kit for Horseradish Peroxidase (both from Vector), respectively.

Recombinant TRAF6-inducible *in vitro* system. This *in vitro* system was as described with slight modifications[16,17]. This used TRAF6 cDNA subcloned into pFAST-Bac-HTa (Gibco BRL) for expression in Sf9 insect cells as six-histidine–tagged proteins. Proteins were purified in accordance with the manufacturer's instructions strictly in the absence of EDTA. For detection of phosphorylation of endogenous TAK1 and IKK, cell extracts (3 mg/ml) prepared in reaction buffer (20 mM Tris-HCl, pH 7.5, and 150 mM NaCl; after sonication) were mixed for 2 h at 30 °C with 2 mM ATP, 2 mM $MgCl_2$, 1 mM dithiothreitol and 0.1 M wild-type ubiquitin or 0.1 M methylated ubiquitin in the presence or absence of 0.1 μM recombinant TRAF6. The reaction was terminated by the addition of SDS-PAGE sample buffer, followed by immunoblot analysis with phosphorylation-specific antibodies as described above.

Statistical analysis. We used the unpaired Student's *t*-test to determine the statistical significance of experimental data.

Note: Supplementary information is available on the Nature Immunology website.

ACKNOWLEDGMENTS

We thank T. Kitamura (The University of Tokyo, Tokyo, Japan) for Plat-E packaging cell lines; D.T. Golenbock (University of Massachusetts Medical School, Worcester, Massachusetts) for the NF-κB-dependent ELAM1 reporter plasmid; J.L. Pomerantz (The Johns Hopkins University School of Medicine, Baltimore, Maryland) for *Card11* expression vectors; J. Inoue (The University of Tokyo, Tokyo, Japan) for the pFastBacHTa-TRAF6 vector; G. Courtois (Hôpital Saint-Louis, Paris, France) for the IKKγ-deficient 1.3E2 cell line; M. Pasparakis (European Molecular Biology Laboratory, Rome, Italy) for MEFs from IKKγ-deficient mice; R.C. Rickert (The Burnham Institute, La Jolla, California) for Cd19-Cre mice; I. Förster (University of Munich, Munich, Germany) for LyzsM-Cre mice; H. Hemmi, T. Yasui and T. Matsunaga for discussions; M. Hashimoto for secretarial assistance; and N. Okita, N. Iwami, N. Fukuda and M. Morita for technical assistance. Supported by Special Coordination Funds; the Ministry of Education, Culture, Sports, Science and Technology; Research Fellowships of the Japan Society for the Promotion of Science for Young Scientists; The Uehara Memorial Foundation; The Naito Foundation and The Junior Research Associate from RIKEN; and Exploratory Research for Advanced Technology, Japan Science and Technology Agency.

AUTHOR CONTRIBUTIONS

All authors contributed to data analysis, experimental design, critical discussions and manuscript preparation; M.Y did all experimental studies; T.O. and Y.M. purified recombinant TRAF6; K.T. generated Ubc13-deficient mice; S.S. and S.U. prepared whole-cell extracts; T.S., N.Y. and S.Y. designed retroviral vectors; H.S. prepared antibodies; K.J.I., T.K. and O.T. played a pivotal role in discussions; and S.A. supervised all work.

COMPETING INTERESTS STATEMENT

The authors declare that they have no competing financial interests.

Published online at http://www.nature.com/natureimmunology/
Reprints and permissions information is available online at http://npg.nature.com/reprintsandpermissions/

1. Ghosh, S. & Karin, M. Missing pieces in the NF-κB puzzle. *Cell* **109**, S81–S96 (2002).
2. Weil, R. & Israel, A. T-cell-receptor- and B-cell-receptor-mediated activation of NF-κB in lymphocytes. *Curr. Opin. Immunol.* **16**, 374–381 (2004).
3. Chang, L. & Karin, M. Mammalian MAP kinase signalling cascades. *Nature* **410**, 37–40 (2001).

4. Akira, S. & Takeda, K. Toll-like receptor signalling. *Nat. Rev. Immunol.* **4**, 499–511 (2004).
5. Kobayashi, T., Walsh, M.C. & Choi, Y. The role of TRAF6 in signal transduction and the immune response. *Microbes Infect.* **6**, 1333–1338 (2004).
6. Chung, J.Y., Park, Y.C., Ye, H. & Wu, H. All TRAFs are not created equal: common and distinct molecular mechanisms of TRAF-mediated signal transduction. *J. Cell Sci.* **115**, 679–688 (2002).
7. Lin, X. & Wang, D. The roles of CARMA1, Bcl10, and MALT1 in antigen receptor signaling. *Semin. Immunol.* **16**, 429–435 (2004).
8. Ruland, J. *et al.* Bcl10 is a positive regulator of antigen receptor-induced activation of NF-κB and neural tube closure. *Cell* **104**, 33–42 (2001).
9. Ruland, J., Duncan, G.S., Wakeham, A. & Mak, T.W. Differential requirement for Malt1 in T and B cell antigen receptor signaling. *Immunity* **19**, 749–758 (2003).
10. Jun, J.E. *et al.* Identifying the MAGUK protein Carma-1 as a central regulator of humoral immune responses and atopy by genome-wide mouse mutagenesis. *Immunity* **18**, 751–762 (2003).
11. Hara, H. *et al.* The MAGUK family protein CARD11 is essential for lymphocyte activation. *Immunity* **18**, 763–775 (2003).
12. Egawa, T. *et al.* Requirement for CARMA1 in antigen receptor-induced NF-κB activation and lymphocyte proliferation. *Curr. Biol.* **13**, 1252–1258 (2003).
13. Ruefli-Brasse, A.A., French, D.M. & Dixit, V.M. Regulation of NF-κB-dependent lymphocyte activation and development by paracaspase. *Science* **302**, 1581–1584 (2003).
14. Newton, K. & Dixit, V.M. Mice lacking the CARD of CARMA1 exhibit defective B lymphocyte development and impaired proliferation of their B and T lymphocytes. *Curr. Biol.* **13**, 1247–1251 (2003).
15. Sun, L., Deng, L., Ea, C.K., Xia, Z.P. & Chen, Z.J. The TRAF6 ubiquitin ligase and TAK1 kinase mediate IKK activation by BCL10 and MALT1 in T lymphocytes. *Mol. Cell* **14**, 289–301 (2004).
16. Deng, L. *et al.* Activation of the IκB kinase complex by TRAF6 requires a dimeric ubiquitin-conjugating enzyme complex and a unique polyubiquitin chain. *Cell* **103**, 351–361 (2000).
17. Wang, C. *et al.* TAK1 is a ubiquitin-dependent kinase of MKK and IKK. *Nature* **412**, 346–351 (2001).
18. Shim, J.H. *et al.* TAK1, but not TAB1 or TAB2, plays an essential role in multiple signaling pathways *in vivo. Genes Dev.* **19**, *2668–2681 (2005).*
19. Sato, S. *et al.* Essential function for the kinase TAK1 in innate and adaptive immune responses. *Nat. Immunol.* **6**, 1087–1095 (2005).
20. Spence, J., Sadis, S., Haas, A.L. & Finley, D. A ubiquitin mutant with specific defects in DNA repair and multiubiquitination. *Mol. Cell. Biol.* **15**, 1265–1273 (1995).
21. Pickart, C.M. & Fushman, D. Polyubiquitin chains: polymeric protein signals. *Curr. Opin. Chem. Biol.* **8**, 610–616 (2004).
22. Hofmann, R.M. & Pickart, C.M. Noncanonical MMS2-encoded ubiquitin-conjugating enzyme functions in assembly of novel polyubiquitin chains for DNA repair. *Cell* **96**, 645–653 (1999).
23. Muralidhar, M.G. & Thomas, J.B. The *Drosophila* bendless gene encodes a neural protein related to ubiquitin-conjugating enzymes. *Neuron* **11**, 253–266 (1993).
24. Zhou, H. *et al.* Bcl10 activates the NF-κB pathway through ubiquitination of NEMO. *Nature* **427**, 167–171 (2004).
25. Zhou, R. *et al.* The role of ubiquitination in *Drosophila* innate immunity. *J. Biol. Chem.* **280**, 34048–34055 (2005).
26. Andersen, P.L. *et al.* Distinct regulation of Ubc13 functions by the two ubiquitin-conjugating enzyme variants Mms2 and Uev1A. *J. Cell Biol.* **170**, 745–755 (2005).
27. Zhou, H., Du, M.Q. & Dixit, V.M. Constitutive NF-κB activation by the t(11;18)(q21;q21) product in MALT lymphoma is linked to deregulated ubiquitin ligase activity. *Cancer Cell* **7**, 425–431 (2005).
28. Habelhah, H. *et al.* Ubiquitination and translocation of TRAF2 is required for activation of JNK but not of p38 or NF-κB. *EMBO J.* **23**, 322–332 (2004).
29. Kobayashi, N. *et al.* Segregation of TRAF6-mediated signaling pathways clarifies its role in osteoclastogenesis. *EMBO J.* **20**, 1271–1280 (2001).
30. Gohda, J., Matsumura, T. & Inoue, J. Cutting edge: TNFR-associated factor (TRAF) 6 is essential for MyD88-dependent pathway but not toll/IL-1 receptor domain-containing adaptor-inducing IFN-β (TRIF)-dependent pathway in TLR signaling. *J. Immunol.* **173**, 2913–2917 (2004).
31. Xue, L. *et al.* Defective development and function of Bcl10-deficient follicular, marginal zone and B1 B cells. *Nat. Immunol.* **4**, 857–865 (2003).
32. Hayden, M.S. & Ghosh, S. Signaling to NF-κB. *Genes Dev.* **18**, 2195–2224 (2004).
33. Chen, Z.J. Ubiquitin signalling in the NF-κB pathway. *Nat. Cell Biol.* **7**, 758–765 (2005).
34. Carter, A.B., Monick, M.M. & Hunninghake, G.W. Both Erk and p38 kinases are necessary for cytokine gene transcription. *Am. J. Respir. Cell Mol. Biol.* **20**, 751–758 (1999).
35. Scherle, P.A. *et al.* Inhibition of MAP kinase kinase prevents cytokine and prostaglandin E2 production in lipopolysaccharide-stimulated monocytes. *J. Immunol.* **161**, 5681–5686 (1998).
36. Zhang, Y. *et al.* Regulation of innate and adaptive immune responses by MAP kinase phosphatase 5. *Nature* **430**, 793–797 (2004).
37. Shinohara, H. *et al.* PKC beta regulates BCR-mediated IKK activation by facilitating the interaction between TAK1 and CARMA1. *J. Exp. Med.* **202**, 1423–1431 (2005).
38. Shi, C.S. & Kehrl, J.H. Tumor necrosis factor (TNF)-induced germinal center kinase-related (GCKR) and stress-activated protein kinase (SAPK) activation depends upon the E2/E3 complex Ubc13-Uev1A/TNF receptor-associated factor 2 (TRAF2). *J. Biol. Chem.* **278**, 15429–15434 (2003).
39. Geetha, T., Kenchappa, R.S., Wooten, M.W. & Carter, B.D. TRAF6-mediated ubiquitination regulates nuclear translocation of NRIF, the p75 receptor interactor. *EMBO J.* **24**, 3859–3868 (2005).
40. Courtois, G., Whiteside, S.T., Sibley, C.H. & Israel, A. Characterization of a mutant cell line that does not activate NF-κB in response to multiple stimuli. *Mol. Cell. Biol.* **17**, 1441–1449 (1997).
41. Krappmann, D., Patke, A., Heissmeyer, V. & Scheidereit, C. B-cell receptor- and phorbol ester-induced NF-κB and c-Jun N-terminal kinase activation in B cells requires novel protein kinase C's. *Mol. Cell. Biol.* **21**, 6640–6650 (2001).
42. Leonardi, A., Chariot, A., Claudio, E., Cunningham, K. & Siebenlist, U. CIKS, a connection to IκB kinase and stress-activated protein kinase. *Proc. Natl. Acad. Sci. USA* **97**, 10494–10499 (2000).
43. Li, X. *et al.* Act1, an NF-κB-activating protein. *Proc. Natl. Acad. Sci. USA* **97**, 10489–10493 (2000).
44. Qian, Y. *et al.* Act1, a negative regulator in CD40- and BAFF-mediated B cell survival. *Immunity* **21**, 575–587 (2004).
45. Pasparakis, M., Schmidt-Supprian, M. & Rajewsky, K. IκB kinase signaling is essential for maintenance of mature B cells. *J. Exp. Med.* **196**, 743–752 (2002).
46. Li, Z.W., Omori, S.A., Labuda, T., Karin, M. & Rickert, R.C. IKKβ is required for peripheral B cell survival and proliferation. *J. Immunol.* **170**, 4630–4637 (2003).
47. Chen, Z. *et al.* Signal-induced site-specific phosphorylation targets IκBα to the ubiquitin-proteasome pathway. *Genes Dev.* **9**, 1586–1597 (1995).
48. Duncan, L.M. *et al.* Lysine-63-linked ubiquitination is required for endolysosomal degradation of class I molecules. *EMBO J.* **25**, 1635–1645 (2006).
49. Yamamoto, M. *et al.* Role of adaptor TRIF in the MyD88-independent toll-like receptor signaling pathway. *Science* **301**, 640–643 (2003).
50. Singhirunnusorn, P., Suzuki, S., Kawasaki, N., Saiki, I. & Sakurai, H. Critical roles of threonine 187 phosphorylation in cellular stress-induced rapid and transient activation of transforming growth factor-β-activated kinase 1 (TAK1) in a signaling complex containing TAK1-binding protein TAB1 and TAB2. *J. Biol. Chem.* **280**, 7359–7368 (2005).
51. Yamaoka, S. *et al.* Complementation cloning of NEMO, a component of the IκB kinase complex essential for NF-κB activation. *Cell* **93**, 1231–1240 (1998).
52. Schmidt-Supprian, M. *et al.* NEMO/IKKγ-deficient mice model incontinentia pigmenti. *Mol. Cell* **5**, 981–992 (2000).
53. Rickert, R.C., Roes, J. & Rajewsky, K. B lymphocyte-specific, Cre-mediated mutagenesis in mice. *Nucleic Acids Res.* **25**, 1317–1318 (1997).
54. Clausen, B.E., Burkhardt, C., Reith, W., Renkawitz, R. & Forster, I. Conditional gene targeting in macrophages and granulocytes using *LysM*cre mice. *Transgenic Res.* **8**, 265–277 (1999).
55. Yamamoto, M. *et al.* TRAM is specifically involved in the Toll-like receptor 4-mediated MyD88-independent signaling pathway. *Nat. Immunol.* **4**, 1144–1150 (2003).
56. Pomerantz, J.L., Denny, E.M. & Baltimore, D. CARD11 mediates factor-specific activation of NF-κB by the T cell receptor complex. *EMBO J.* **21**, 5184–5194 (2002).
57. Yamamoto, M. *et al.* Regulation of Toll/IL-1-receptor-mediated gene expression by the inducible nuclear protein IκBζ. *Nature* **430**, 218–222 (2004).

GASTROENTEROLOGY 2007;132:208–220

Reciprocal Targeting of Hath1 and β-Catenin by Wnt Glycogen Synthase Kinase 3β in Human Colon Cancer

KIICHIRO TSUCHIYA, TETSUYA NAKAMURA, RYUICHI OKAMOTO, TAKANORI KANAI, and MAMORU WATANABE

Department of Gastroenterology and Hepatology, Graduate School, Tokyo Medical and Dental University, Tokyo, Japan

Background & Aims: **The transcription factor Hath1 plays a crucial role in the differentiation program of the human gut epithelium. The present study was conducted to investigate the molecular mechanism of Hath1 expression and its close association with β-catenin/glycogen synthase kinase 3β (GSK3β) under the Wnt pathway in human colonocytes.** ***Methods:*** **Tissue distribution of Hath1 messenger RNA in human tissues was examined by Northern blot. Stability of Hath1 protein was analyzed by expression of FLAG-tagged Hath1 in human cell lines. Targeting of Hath1 protein by GSK3β was determined by specific inhibition of GSK-3β function. Expression of Hath1 protein in colorectal cancers was examined by immunohistochemistry.** ***Results:*** **Hath1 messenger RNA expression was confined to the lower gastrointestinal tract in human adult tissues. In colon cancer cells, although Hath1 messenger RNA was also detected, Hath1 protein was positively degradated by proteasome-mediated proteolysis. Surprisingly, the GSK3β-dependent protein degradation was switched between Hath1 and β-catenin by Wnt signaling, leading to the dramatic alteration of cell status between proliferation and differentiation, respectively. Hath1 protein was detected exclusively in normal colon tissues but not in cancer tissues, where nuclear-localized β-catenin was present.** ***Conclusions:*** **The present study suggests a novel function of the canonical Wnt signaling in human colon cancer cells, regulating cell proliferation and differentiation by GSK3β-mediated, reciprocal degradation of β-catenin or Hath1, respectively, which further emphasizes the importance of aberrant Wnt signaling in colonocyte transformation.**

BASIC

The gut epithelium undergoes continual renewal throughout adult life, maintaining the proper architecture and function of the intestinal crypts. This process involves highly coordinated regulation of the induction of cellular differentiation and the cessation of proliferation, and vice versa.[1–3] The intestinal epithelium consists of cells of 4 lineages: goblet cells, enteroendocrine cells, Paneth cells, and enterocytes.[4] Cellular differentiation into the former 3 lineages is believed to be regulated by a basic helix-loop-helix transcription factor called "Math1" in mice and "Hath1" in humans (officially termed as "ATOH1"). Math1 and Hath1 are known to play crucial roles in differentiation of various cells in other tissues, such as dorsal interneurons in the spinal cord,[5] granule cells in the cerebellum,[6] Merkel cells in the skin,[7] and inner hair cells in the auditory systems.[8]

In mice intestine, the *Math1* gene promotes the differentiation of epithelial cells to secretory lineage cells without affecting absorptive cell differentiation and is expressed in Ki-67–positive proliferating cells of the crypt, indicating a role of Math1 at an early stage of lineage commitment.[9] Expression of Math1 seems to be regulated at its transcriptional level, because forced expression of Notch intracellular domain in murine intestinal epithelial cells causes a decrease of Math1 messenger RNA (mRNA) expression and subsequent depletion of goblet cells in vivo.[10] Conversely, depletion of Hes1, another basic helix-loop-helix transcription factor known as a downstream target of Notch intracellular domain, up-regulates Math1 mRNA expression in murine intestine.[11] Thus, it is likely that *Math1* gene expression is regulated at the mRNA level by Notch signaling, leading to subsequent control of intestinal epithelial cell lineage decision of the crypt cells. It was recently reported that Hath1, a human homologue of Math1, up-regulates gastric mucin gene expression in gastric cells[12]; however, the regulation of Hath1 expression is less understood in human intestine.

The canonical Wnt signaling is another signaling pathway known to regulate cell differentiation and proliferation of the intestinal crypt cells.[13] It is believed that Wnt proteins induce inactivation of glycogen synthase kinase 3β (GSK3β), a component of the so-called destruction complex that also contains adenomatous polyposis coli (APC) and Axin, and the resultant dephosphorylation and stabilization of its substrate β-catenin leads to the transcription of genes targeted by the nuclear β-catenin/

Abbreviations used in this paper: APC, adenomatous polyposis coli; EGFP, enhanced green fluorescent protein; G3PDH, glyceraldehyde-3-phosphate dehydrogenase; GSK3β, glycogen synthase kinase 3b; RIPA, radioimmunoprecipitation assay; RT-PCR, reverse-transcription polymerase chain reaction; SDS, sodium dodecyl sulfate; siRNA, small interfering RNA; TCF, T-cell factor.

0016-5085/07/$32.00
doi:10.1053/j.gastro.2006.10.031

T-cell factor (TCF) complex.[14,15] However, in intestinal cells, it has not been shown whether activation of Wnt signaling simply inactivates general kinase activity of GSK3β or could possibly change the substrate specificity instead of kinase activity, thereby stabilizing the β-catenin protein. Constitutive activation of Wnt signaling is assumed to be essential for both continuous proliferation and maintenance of the undifferentiated state in intestinal stem cells.[16,17] Of note, the biological impact of the Wnt pathway lies in its close association with the carcinogenesis of colorectal cancer. Mutations that perturb the assembly or function of the destruction complex, such as truncation of APC, are present in approximately more than 90% of colorectal tumors. These mutations lead to constitutive activation of Wnt signaling, and the downstream genes that are transcriptionally up-regulated by the β-catenin/TCF complex are implicated in the growth-promoting properties of the tumor cells.[15,18] However, it has not been well understood how constitutive Wnt signaling could maintain colorectal cancer cells at an undifferentiated state.

A previous study reported that inhibition of Wnt signaling in a human colon cancer–derived cell line, HT-29, up-regulated both *Hath1* and *MUC2* gene mRNA expression.[19] This suggested that Hath1 expression may be suppressed at the mRNA level by the aberrant Wnt signaling, thereby maintaining the undifferentiated state of colorectal cancer cells. However, in the same study, it was also suggested that some colorectal cancers did express Hath1 mRNA at an amount comparable to the neighboring normal colon tissue but maintained an undifferentiated state at the same time.

These data prompted us to prove that *Hath1* gene function is regulated by the aberrant Wnt signaling, not only by the mRNA level but also by an unknown posttranscriptional or posttranslational mechanism in human colon cancer cells. Here, we present the evidence that Hath1 protein expression is regulated by Wnt signaling via GSK3β-mediated protein degradation. Our results suggest that the reciprocal regulation of Hath1 and β-catenin protein stability is mediated by GSK3β, which functions as a molecular switch regulating the proliferation and differentiation of colon cancer cells in vitro and in vivo. These results present a novel function of the Wnt-GSK3β pathway and further emphasize the importance of aberrant Wnt signaling in colonocyte transformation.

Materials and Methods

Cell Culture

Human colon cancer–derived SW480, DLD-1, and HT-29 cells and human embryonic kidney-derived 293T cells were grown in Dulbecco's modified Eagle medium (Life Technologies, Grand Island, NY) supplemented with 10% fetal bovine serum and 1% penicillin-streptomycin. In all experiments, 1×10^6 cells were seeded onto 6-cm culture dishes 36 hours before the experiment. All transfection experiments of DNA constructs and small interfering RNA (siRNA) oligonucleotides were performed by using TransIT transfection reagent (Mirus, Madison, WI) according to the manufacturer's instructions.

DNA Constructs

pcDNA3-Myc-ubiquitin[20] was a kind gift from Dr K. Tanaka (Tokyo Metropolitan Institute, Tokyo, Japan). pMX-IRES-GFP[21] was a kind gift from Dr T. Kitamura (University of Tokyo, Tokyo, Japan). Series of expression vectors encoding mutants for *APC* genes (pCS2-APC2, -APC3, and -APC25)[22] and a pRL5-Wnt1[23] were kind gifts from Dr H Shibuya (Tokyo Medical and Dental University, Tokyo, Japan). Expression plasmids encoding N-terminally Flag-tagged WT-Hath1 (pCMV-Flag-WT-Hath1) or enhanced green fluorescent protein (EGFP) (pCMV-Flag-EGFP) were generated by inserting the polymerase chain reaction (PCR)-amplified *Hath1* gene or *EGFP* gene, respectively, into the *Eco*RI/*Bam*HI site of a pCMV-Flag vector (Stratagene, La Jolla, CA) in frame. Plasmids for various mutants that lack either the N- or C-terminal region of Hath1 (N1-5, C1, and C2 mutants; Figure 3*A*) and the mutant 54/58SA-Hath1, in which both 54S and 58S are substituted to alanines, were constructed by PCR-mediated mutagenesis by using pCMV-Flag-WT-Hath1 as a starting material. pMX-Flag-WT-Hath1-IRES-GFP was generated by inserting a fragment encoding the N-terminally Flag-tagged *Hath1* gene, which was amplified by PCR using pCMV-Flag-WT-Hath1 as a template, into the pMX-IRES-GFP vector. A reporter plasmid E-box Luc was generated by inserting a 77–base pair oligonucleotide containing 7 repeats of the E-box (kE sites) (AGGCAGGTGGC) into an *Sma*I site of the pTA-Luc vector (Clontech, Mountain View, CA). Reporter plasmids TOPflash and FOPflash were obtained from Upstate Biotechnology (Charlottesville, VA). All plasmids constructed were verified by sequencing.

Immunoblottings and Immunoprecipitations

Cells were transfected with 1 μg of pCMV-Flag vector (control), pCMV-Flag-EGFP, pCMV-Flag-Hath1, or various mutants of pCMV-Flag-Hath1. In cotransfection experiments, 1 μg of either pcDNA3-Myc-ubiquitin or one of the expression plasmids for mutant APC (pCS2-APC2, -APC25, or -APC3) or pRL5-Wnt1 was transfected along with 1 μg of pCMV-Flag vector (control) or pCMV-Flag-Hath1. In each cotransfection experiment, the total amount of DNA was equalized by adding the appropriate amount of empty expression vector. After 12 hours of transfection, cells were cultured for 12 hours under the usual conditions or in the presence of 10 μmol/L lactacystin (Calbiochem, San Diego, CA), 10 μmol/L MG132 (Calbiochem), 5 μmol/L calpain inhibitor (Calbiochem),

100 μmol/L chloroquine (Sigma-Aldrich, St Louis, MO), 100 μmol/L RO-31-8220 (Calbiochem), 100 μmol/L staurosporine (Calbiochem), 1 μmol/L UO126 (Calbiochem), 30 mmol/L LiCl (Sigma-Aldrich), 30 mmol/L kenpaullone (Calbiochem), or 5 μmol/L BIO (Calbiochem).

For siRNA experiments, SW480 cells were transfected with 100 nmol/L siRNA oligonucleotide along with 1 μg of pCMV-Flag-WT-Hath1 for 12 hours, cultured for an additional 12 hours under the usual conditions, and then treated with MG132 or left untreated for 12 hours. A siRNA oligonucleotide specific for human GSK3β was obtained from Santa Cruz Biotechnology (Santa Cruz, CA), and a negative control (nonsense siRNA) oligonucleotide was synthesized as described elsewhere.[24] After transfection, cells were harvested, washed with phosphate-buffered saline (PBS) once, and incubated on ice for 15 minutes in 1% sodium dodecyl sulfate (SDS)-containing radioimmunoprecipitation assay (RIPA) buffer (10 mM Tris-HCl [pH 8.0], 1% Triton X-100, 1% SDS, 0.1% sodium deoxycholate, 1 mmol/L EDTA, 0.5 mmol/L ethylene glycol-bis(β-aminoethyl ether)-*N,N,N′,N′*-tetraacetic acid, and 140 mmol/L NaCl). After brief sonication of the lysates to shear genomic DNA, the samples were centrifuged for 20 minutes and the supernatant was used as whole cell extract. The protein concentration in each sample was determined by using protein assay reagent (Pierce, Rockford, IL). For immunoblotting, 50 μg or 100 μg of whole cell extract was separated in 12% SDS-polyacrylamide gels, transferred to polyvinylidene difluoride membranes, blocked, and probed according to standard procedures.[24] The following antibodies and dilutions were used: mouse anti-Flag M2 (Sigma Chemical Co, St Louis, MO), 1:5000; mouse anti-dephospho-β-catenin (Alexis, San Diego, CA), 1:500; mouse anti-GSK3 (Calbiochem), 1:1000; rabbit anti-USF2 (loading control for the amount of nuclear proteins; Santa Cruz Biotechnology), 1:1000; and mouse anti-β-actin (loading control for the whole cell extracts; Sigma Chemical Co), 1:5000. Horseradish peroxidase-conjugated secondary antibodies were used for mouse (Amersham Biosciences UK, Buckinghamshire, England) and rabbit immunoglobulin G (Cell Signaling Technology, Danvers, MA). Blots were visualized with the ECL Plus System (Amersham Biosciences UK) by using a Lumi-Imager F1 system (Roche Diagnostics, Rotkreutz, Switzerland). For immunoprecipitation assays, 300 μg of whole cell extract in 1% SDS-containing RIPA buffer was diluted with 9 vol of non-SDS-containing RIPA buffer to give an SDS concentration of 0.1%, and then the total volume was adjusted to 1 mL by adding an appropriate amount of 0.1% SDS-containing RIPA buffer. The lysates were precleared by incubation with 40 μL of protein G/Sepharose (50% slurry in 0.1% SDS-RIPA buffer) for 1 hour, and then the supernatants were incubated with 1 μg of anti-Flag M2 antibody (Sigma Chemical Co) overnight. A 40-μL aliquot of 50% protein G/Sepharose slurry was added to each sample and incubated for 2 hours at 4°C. Precipitates were washed 3 times in 0.1% SDS-containing RIPA buffer, resolved by SDS/polyacrylamide gel electrophoresis, and analyzed by immunoblotting using a mouse anti-myc antibody (Invitrogen, Carlsbad, CA) at 1:1000 dilution. Protein visualization was performed as described previously.

Semiquantitative Reverse-Transcription PCR and Northern Blotting

Total RNA was isolated by using TRIzol reagent (Invitrogen). Aliquots of 5 μg of total RNA were used for complementary DNA synthesis in 21 μL of reaction volume by using oligo dT primers. One microliter of complementary DNA was amplified with 0.25 U of LA Taq polymerase (Takara Bio, Otsu, Japan) in a 25-μL reaction. Sense and antisense primers and the cycle numbers for the amplification of each gene were as follows: sense Flag, 5′-CACCATGGATTACAAGGATGACGACGAT-3′ and antisense Hath1, 5′-TTGCCCGCGCCCCCTTCATAG-3′ for the fragment covering the region for Flag-Hath1 (20 cycles); sense Flag, 5′-CACCATGGATTACAAGGATGACGACGAT-3′ (common for the S primer for the Flag-Hath1 fragment) and antisense Flag-EGFP, 5′-AGGATGTTGCCGTCCTCC-3′ for Flag-EGFP (20 cycles); sense GSK3β, 5′-ATCTTAATCTGGTGCTGGACTATGT-3′ and antisense GSK3β, 5′-TTGAGTGGTGAAGTTGAAGAGTGCA-3′ for GSK3β (25 cycles); sense MUC2, 5′-CTGCACCAAGACCGTCCTCATG-3′ and antisense MUC2, 5′-GCAAGGACTGAACAAAGACTCAGAC-3′ for MUC2 (25 cycles); sense c-Myc, 5′-CTTCTGCTGGAGGCCACAGCAAACCTCCTC-3′ and antisense-c-Myc, 5′-CCAACTCCGGGATCTGGTCACGCAGGG -3′ for c-Myc (25 cycles); sense Hath1, 5′-AAGACGTTGCAGAAGAGACCCG-3′ and antisense Hath1, 5′- TTGCCCGCGCCCCCTTCATAG-3′ (common for the antisense primer for Flag-Hath1 fragment) for endogenous Hath1 (25 cycles); and sense glyceraldehyde-3-phosphate dehydrogenase (G3PDH), 5′-TGAAGGTCGGAGTCAACGGATTTGGT-3′ and antisense G3PDH, 5′-CATGTGGGCCATGAGGTCCACCAC-3′ for glyceraldehyde-3-phosphate dehydrogenase (17 cycles). The amplification for each gene was logarithmic under these conditions. PCR products were separated on 1.5% agarose gels, stained with ethidium bromide, and visualized with a Lumi-Imager F1 (Roche Diagnostics).

Expression levels of Hath1 mRNA in human tissues were analyzed by using 2 human multiple tissue blots (BioChain Institute, Hayward, CA). The complementary DNA probe corresponding to nucleotides +1/+749 for the *Hath1* gene was generated by reverse-transcription (RT)-PCR from an RNA sample obtained from human colonic tissues. The probe for G3PDH was also generated by RT-PCR. The probes were labeled with [α-32P]deoxycytidine triphosphate by random priming using RediPrime II (Amersham Biosciences UK) according to the

manufacturer's instructions. Hybridization was performed in Ultra Hyb solution (Ambion, Austin, TX) at 42°C overnight for Hath1 and at 55°C for 2 hours for β-actin. Visualization of the hybridized signals was conducted with the BAS-2000 image analyzing system (Fuji Film, Tokyo, Japan).

Reporter Assays

SW480 cells were transiently transfected with 10 ng of renilla luciferase reporter plasmid pRL-TK-Luc (Promega) along with 100 ng of either TOPflash, FOPflash, or an E-box-Luc reporter plasmid. One microgram of the expression plasmid pCMV-Flag-WT-Hath1 or its empty control, and the same amount of pCS2-APC2 or its empty control, were also cotransfected, keeping the total amount of plasmid per transfection constant. Transfections of 293T cells were performed identically, except for substituting the pCS2-APC2 with the pRL5-Wnt1 and the pCS2 vector with the pRL5 vector, respectively. After 12 hours of transfection, cells were cultured for 24 hours and lysed by 3 cycles of freezing and thawing. Firefly luciferase activity was normalized with renilla luciferase activity in each sample by using the Dual Luciferase Kit (Promega). The E-box-dependent luciferase activities were shown as arbitrary units normalized by renilla luciferase activity, and the β-catenin/TCF-dependent luciferase activities were shown as a ratio of TOPflash and FOPflash.

Immunocytochemistry

SW480 cells were cotransfected on a sterile glass coverslip with 1 μg of a bicistronic expression vector pMX-Flag-Hath1-IRES-GFP or its empty control together with 1 μg of a pCS2-APC2 or pCS2 vector as indicated. Twelve hours after transfection, cells were fixed with 4.0% paraformaldehyde, rinsed twice with PBS, and permeabilized with 0.2% Triton X-100 in PBS, followed by incubation for 1 hour in 3% bovine serum albumin-containing PBS to block nonspecific antibody binding. The samples were incubated for 3 hours at 37°C with either mouse anti-Flag antibody (1 μg/mL) or mouse anti-MUC2 antibody (1 μg/mL, Ccp58; Santa Cruz Biotechnology), washed twice with PBS, and then incubated for 1 hour at 37°C with Alexa 594-conjugated anti-mouse fluorescent secondary antibodies (Molecular Probes, Eugene, OR). The cells were also counterstained with 4′,6-diamidino-2-phenylindole (Vector Laboratories, Burlingame, CA) to visualize nuclei. The samples were washed 3 times with PBS and analyzed with an epifluorescence microscope (BX-50; Olympus, Tokyo, Japan) equipped with a PDMC device camera (Polaroid, Waltham, MA) for coexistence of the fluorescent signals of the secondary antibodies (Flag-Hath1 or MUC2 protein) and green fluorescent protein, the latter of which is translated from the IRES element fused downstream of the coding region for Flag-Hath1 protein. Images were processed in Adobe Photoshop software (Adobe Systems Inc, San Jose, CA).

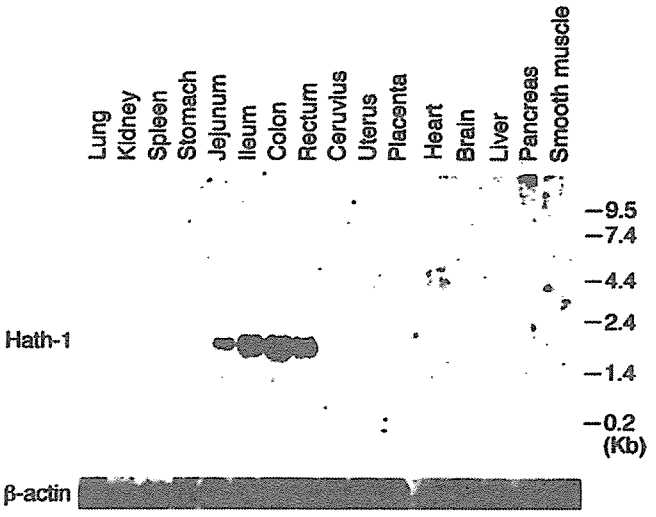

Figure 1. Expression of Hath1 mRNA is confined to the lower gastrointestinal tract. Hath1 mRNA expression in various adult human tissues was analyzed by Northern blotting by using a complementary DNA probe corresponding to nucleotides +1/+749 of the *Hath1* gene. Hybridization with a probe for β-actin is shown as a loading control. Hath1 mRNA is indeed exclusively expressed in the gastrointestinal tract of the human adult body. Moreover, the amount of Hath1 mRNA expression within the gastrointestinal tract increases as it reaches downward to the anal verge, where the population of secretory lineage epithelial cells is also increased.

Immunohistochemistry

Normal and cancerous colonic mucosae were obtained from 4 patients with colorectal cancer who underwent colectomy. Written informed consent was obtained from all patients, and these experiments were approved by the Tokyo Medical and Dental University Hospital Ethics Committee on Human Subjects. Immunohistochemistry for β-catenin was performed as described elsewhere,[25] using anti-β-catenin antibody (BD Transduction, San Diego, CA) and the standard ABC method (Vectastain; Vector Laboratories). Staining was developed by addition of diaminobenzidine (Vector Laboratories). Hath-1 antibody was generated by immunizing rabbits with Hath-1 peptide (247–265). Samples were fixed with 4% paraformaldehyde and subjected for staining using a TSA Signal Amplifying Kit (Molecular Probes) following the manufacturer's instructions. Staining was developed by addition of Alexa 488-conjugated tyramide. Sections were also counterstained with 4′,6-diamidino-2-phenylindole (Vector Laboratories) to visualize nuclei. Stained samples were analyzed with an epifluorescence microscope (BX-50; Olympus) equipped with a PDMC device camera (Polaroid).

Results

Expression of Hath1 mRNA Is Confined to the Lower Gastrointestinal Tract

The mRNA expression of Math1 and Hath1 is reported to be confined to the gastrointestinal tract in adult mice[26] and humans,[19] respectively. However, precise analysis of the expression of Hath1 mRNA within the gastrointestinal tract has never been reported. Thus, we compared mRNA expression of Hath1 in each section of the adult human gastrointestinal tract by Northern blotting. Results revealed that Hath1 mRNA is indeed exclusively expressed in the gastrointestinal tract, from the jejunum to the rectum (Figure 1). Moreover, the amount of Hath1 mRNA expression was significantly increased in the colon, compared with the jejunum or the ileum, where the population of secretory lineage epithelial cells is relatively increased. These results suggested that Hath1 expression is strictly regulated by mRNA expression, at least in the normal adult human body, and may have critical roles especially in the differentiation of colonocytes into secretory lineage cells.

Hath1 Undergoes Proteasome-Mediated Proteolysis in Human Colon Cancer–Derived Cells

To further analyze the functional role of Hath1 in colonocyte differentiation, we first asked whether an overexpression of Hath1 could change any phenotype of human colon-derived epithelial cells. Because the results of the former section suggested that expression of Hath1 mRNA may directly lead to Hath1 protein

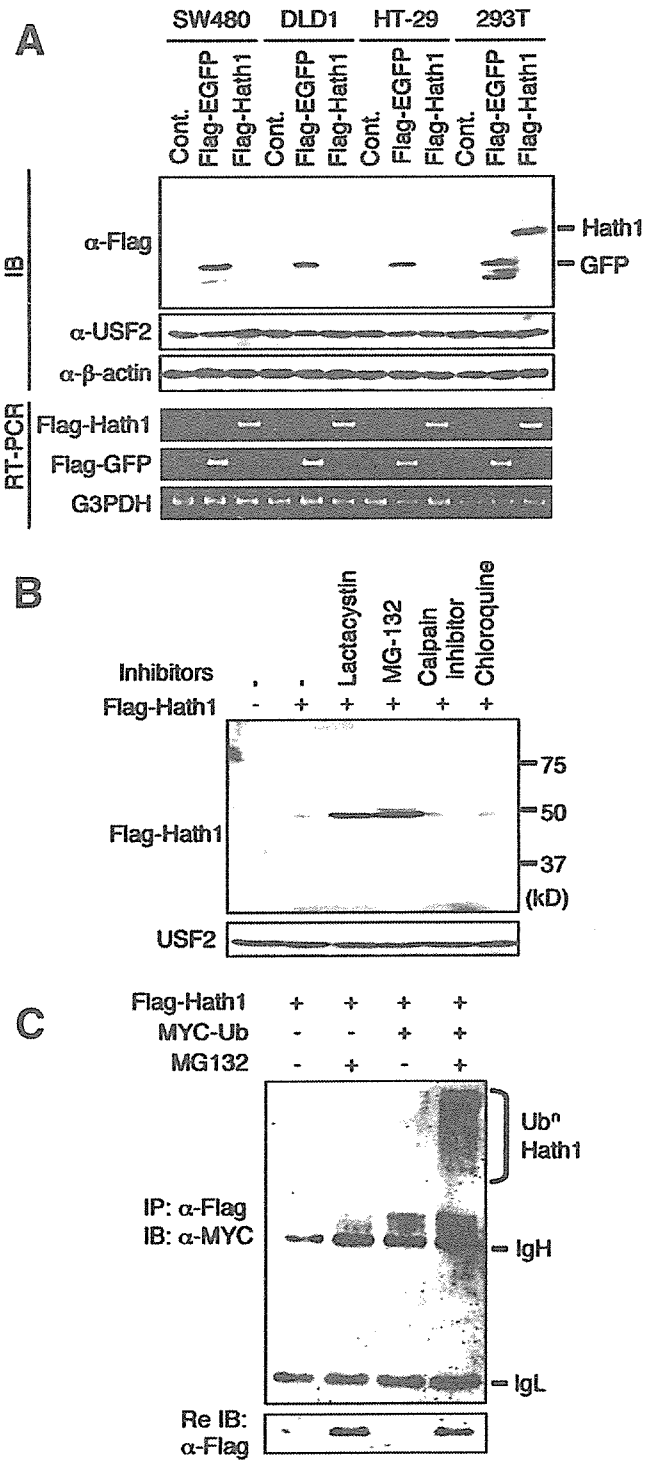

Figure 2. Hath1 undergoes proteasome-mediated proteolysis in human colon cancer–derived cells. (*A*) Hath1 protein expression cannot be detected after introduction of a gene encoding Hath1 in human colon cancer–derived cells. An expression plasmid encoding either Flag-tagged WT-Hath1 (Flag-Hath1), Flag-tagged EGFP (Flag-EGFP), or an empty control (Cont.) was transfected into human colon cancer–derived cell lines (SW480, DLD-1, and HT-29) or a noncolonic cell line (293T). Introduction of the genes was confirmed by semiquantitative RT-PCR, and the expression of the corresponding protein was examined by immunoblot (IB). While Flag-tagged EGFP shows stable expression of both mRNA and protein in every cell line, protein expression of Flag-Hath1 is detectable in 293T cells but not in colon cancer cell lines. Semiquantitative RT-PCR shows an equal amount of Flag-Hath1 mRNA expression in both 293T cells and colon cancer cell lines. (*B*) Hath1 protein is degradated by a proteasome-mediated mechanism in colon cancer cells. Flag-WT-Hath1 (Flag-Hath1) expression vector was transfected into SW480 cells and treated with various inhibitors of cellular proteolytic systems during protein expression. Expression of FLAG-Hath1 protein was examined by immunoblot using anti-Flag antibodies. Only the inhibitors of the proteasome pathway (lactacystin and MG132), but not any other inhibitor of the proteolytic pathway (calpain inhibitor and chloroquine), significantly increased protein expression of FLAG-Hath1. (*C*) Hath1 protein is polyubiquitinated in colon cancer cells. Expression vectors for Flag-Hath1 and Myc-tagged ubiquitin (Myc-Ub) were cotransfected into SW480 cells. Following transfection, cells were treated with or without MG132 during protein expression. The lysates were immunoprecipitated (IP) with anti-Flag antibodies and subjected to immunoblot (IB) using anti-Myc antibodies. Cotransfection of Flag-Hath1 and Myc-Ub, followed by inhibition of the proteasome pathway by MG132, allowed detection of the stabilized, polyubiquitinated FLAG-Hath1 protein by anti-myc antibody. Two bands labeled as IgH and IgL represent heavy chain and light chain of anti-Flag antibody used for immunoprecipitation, respectively. Reprobing the same membrane (Re IB) with anti-FLAG antibody shows efficient immunoprecipitation of FLAG-Hath1 protein only in MG132-treated conditions, because FLAG-Hath1 proteins are readily ubiquitinated and degradated in other conditions.

expression and function to regulate differentiation in colonocytes, we introduced an expression plasmid vector encoding Flag-tagged Hath1 (Flag-WT-Hath1) into various human colon cancer-derived epithelial cell lines. Surprisingly, significant expression of FLAG-Hath1 protein could not be observed in all 3 colon cancer cell lines examined, which were SW480, DLD1, and HT-29. This was not due to low efficiency of transfection or poor sensitivity of the immunoblot, because expression of Flag-EGFP protein could be easily detected by introducing the same amount of the expression plasmid having the same plasmid backbone (Figure 2*A*). Furthermore, semiquantitative RT-PCR showed an equal amount of Flag-Hath1 or Flag-EGFP mRNA expression in every colon cancer cell line, confirming the efficient transfection of the FLAG-Hath1 gene. However, Flag-Hath1 and Flag-EGFP showed equal expression of both mRNA and protein in 293T cells. These results suggested that there might be a posttranscriptional regulation of Hath1 expression involving protein degradation, specifically in colon cancer cells (Figure 2*A*). To confirm the involvement of proteolysis in the significantly decreased expression of Hath1 protein in colon cancer cell lines, we used various pharmacologic inhibitors of the cellular proteolytic system. When SW480 cells were treated with these inhibitors after transfection of Flag-Hath1 expression vectors, inhibitors such as calpain inhibitor or chloroquine had no effect on protein expression of Flag-Hath1 (Figure 2*B*). In sharp contrast, treatment with proteasome inhibitors such as MG132 or lactacystin significantly increased the protein expression of Flag-Hath1, suggesting that Hath1 protein is degradated by the proteasome-mediated proteolysis in colon cancer cells (Figure 2*B*). Because proteasome-mediated proteolysis often requires conjugation of ubiquitins to the target protein,[27,28] we next examined whether Hath1 proteins are ubiquitinated before degradation in

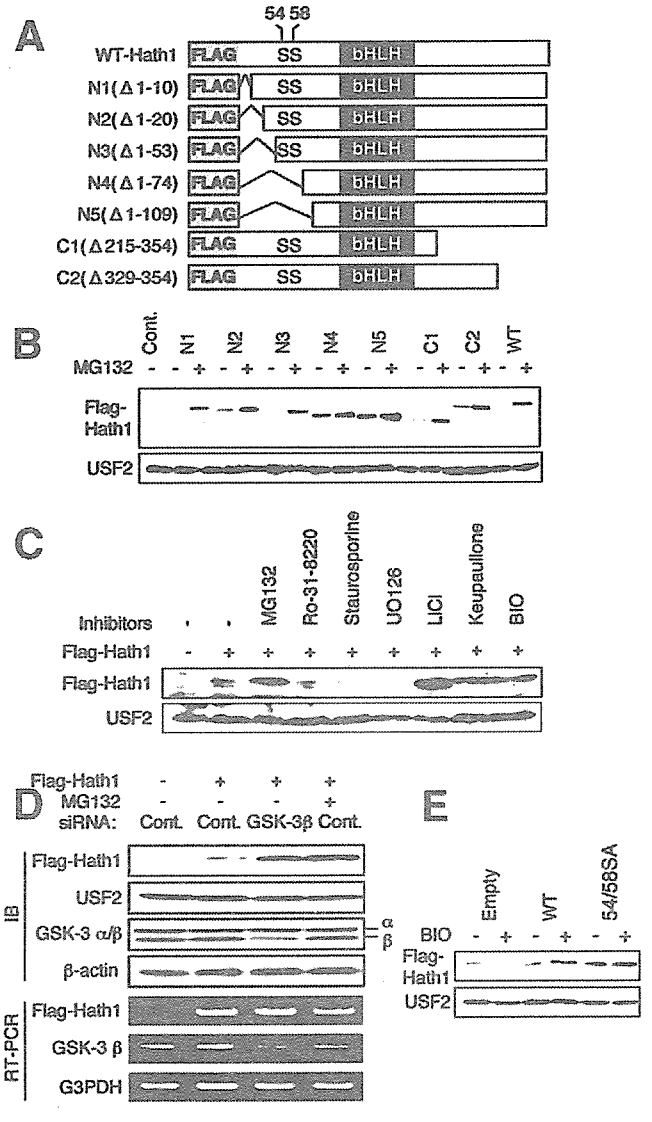

Figure 3. GSK3β-mediated Hath1 proteolysis in colon cancer cells critically requires S54 and S58 of Hath1 protein. (*A*) Schematic representation of various FLAG-tagged Hath1 mutants. Deletion mutants of the N-terminal or C-terminal part of the Hath1 protein are designated as N1–N4 or C1 and C2 mutants. The deleted region of each mutant is designated by amino acid numbers, that is, Δ1–10 designates deletion of amino acid 1–10 of Hath1 protein. The basic helix-loop-helix domain located in the central region as well as 2 serine (S) residues at positions 54 (S54) and 58 (S58) are shown. (*B*) The region consisting of amino acids 54–74 is required for active degradation of Hath1 protein. The wild-type and mutant Hath1 protein shown in *A* were expressed with or without MG132 treatment in SW480 cells. Protein expression was detected by immunoblot using anti-FLAG antibody. N4 and N5 mutant, but not any other wild-type or mutant Hath1 protein, showed no difference in the amount of protein expression between MG132-treated or untreated conditions. (*C*) Proteolysis of Hath1 is suppressed by specific inhibitors of GSK3β in colon cancer cells. Flag-WT-Hath1 was transfected into SW480 cells and treated with various protein kinase inhibitors. Protein expression was detected by immunoblot using anti-FLAG antibody. FLAG-Hath1 protein is stabilized by the proteasome inhibitor (MG132) and kinase inhibitors specific for GSK3β (LiCl, kenpaullone, BIO) but not by other kinase inhibitors (Ro-31-8220, staurosporine, UO126). (*D*) Gene silencing of GSK3β by siRNA increases Hath1 protein expression. An siRNA specific for GSK3β was cotransfected with Flag-WT-Hath1 into SW480 cells. Transfection of a nonsense siRNA served as a control (Cont.). Expression of FLAG-Hath1 and GSK3β was analyzed by semiquantitative RT-PCR and immunoblotting. Transfection of a GSK3β-specific siRNA significantly reduced both mRNA and protein expression of GSK3β. The specific knockdown of GSK3β increased protein expression of cotransfected FLAG-Hath1, which could also be induced up to a similar level by MG132 treatment. (*E*) S54 and S58 are the critical residues for GSK3β-mediated Hath1 proteolysis. An empty vector encoding no protein (*Empty*), or FLAG-tagged, wild-type (WT), or 54/58 SA mutant of Hath1 (54/58SA), in which both S54 and S58 of the Hath1 protein were substituted to alanines, was transfected into SW480 cells. The effect of treatment with a GSK3β-specific inhibitor (BIO) on the expression of each protein in SW480 cells was examined by immunoblot. 54/58 SA mutant of Hath1, but not the WT, showed stable protein expression without BIO treatment. A trace signal examined in the left end of the "Flag-Hath1" blot has been determined to be a nonspecific signal and does not represent expression of a Flag-tagged protein.

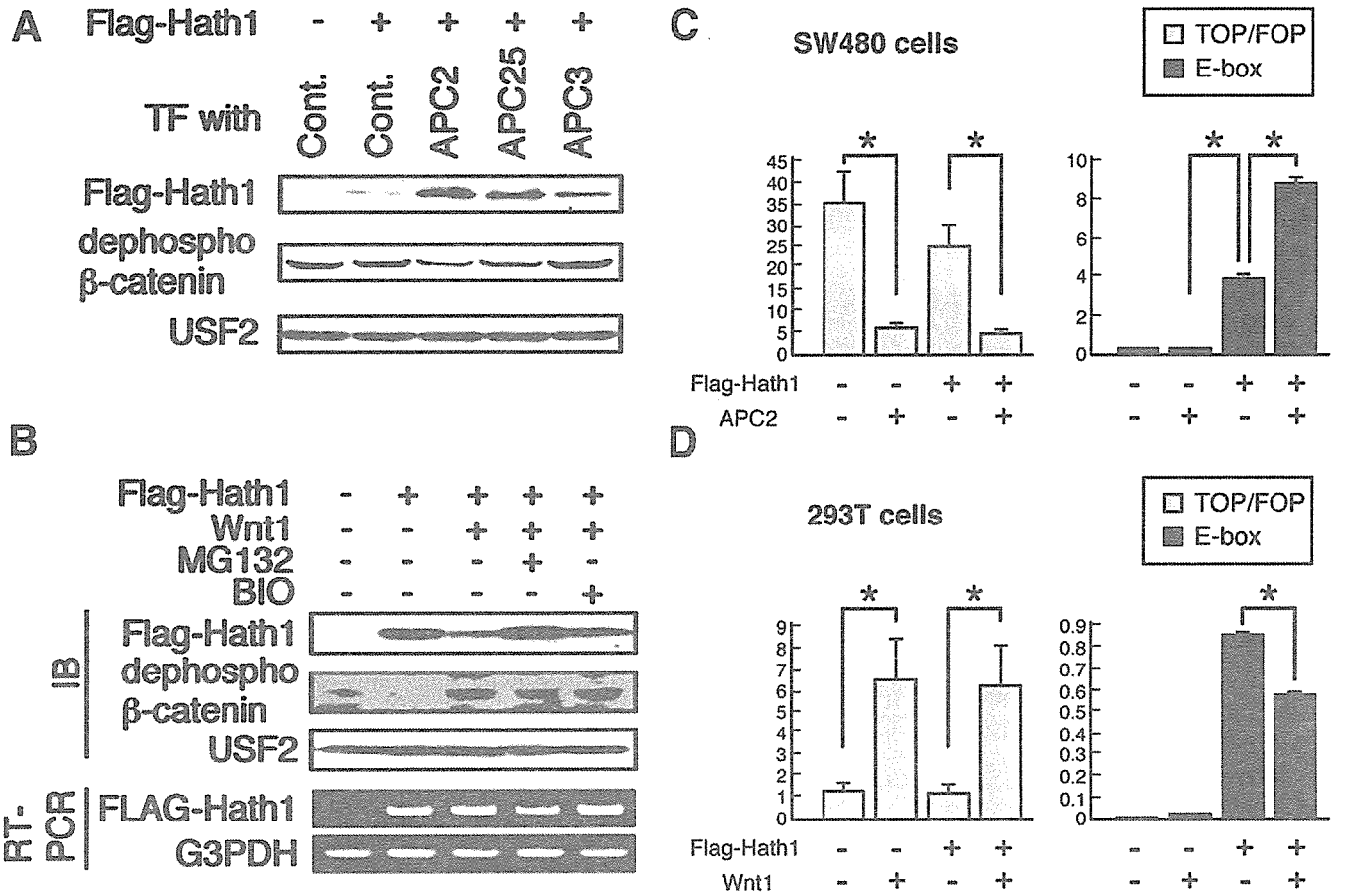

Figure 4. The canonical Wnt pathway reciprocally regulates Hath1 and β-catenin protein stability and downstream transcription activities via GSK3β. (*A*) Suppression of Wnt signaling in colon cancer cells increases expression of Hath1 protein. Flag-WT-Hath1 and APC mutants that are capable (APC2 and APC25) or incapable (APC3) of destabilizing β-catenin were cotransfected into SW480 cells. Cell lysates were subjected to immunoblotting for Flag-Hath1 (anti-Flag) or dephosphorylated β-catenin. Cotransfection of APC2 or APC25, but not of APC3, reduced the amount of dephosphorylated β-catenin protein and conversely increased the amount of Hath1 protein. (*B*) Activation of Wnt signaling induces degradation of Hath1 protein. Expression vectors for Flag-Hath1 and Wnt1 were cotransfected into 293T cells. Cells were cultured with or without MG132 or BIO, and protein expression of Hath1 and dephosphorylated β-catenin was analyzed by immunoblotting (IB). Equivalent transfection of Flag-Hath1 was confirmed by semiquantitative RT-PCR. Expression of Wnt1 in 293T cells induced dephosphorylation of β-catenin protein and also reduced expression of the cotransfected Flag-Hath1 protein (*lane 3*). This reduction of Flag-Hath1 protein is rescued by addition of a proteasome inhibitor (MG132) or a specific inhibitor of GSK3 (BIO). (*C*) Suppression of Wnt signaling in colon cancer cells up-regulates Hath1-mediated, E-box–dependent transcription and reciprocally down-regulates β-catenin/TCF–dependent transcription. Flag-WT-Hath, APC2, and designated reporter constructs were cotransfected into SW480 cells. E-box–dependent luciferase activities were shown as arbitrary units after normalization by renilla luciferase activity, and β-catenin/TCF–dependent luciferase activities are shown as a ratio of TOPflash and FOPflash. *$P < .005$. Transfection of APC2 significantly down-regulated β-catenin/TCF–dependent transcription but conversely up-regulated Hath1-mediated, E-box–dependent transcription in SW480 cells. (*D*) Activation of Wnt signaling in 293T cells down-regulates Hath1-mediated, E-box–dependent transcription and reciprocally up-regulates β-catenin/TCF–dependent transcription. Flag-WT-Hath, Wnt1, and designated reporter constructs were cotransfected into 293T cells. E-box– and β-catenin/TCF–dependent transcriptional activities were measured as described in the former section. *$P < .005$. Transfection of Wnt1 significantly up-regulated β-catenin/TCF–dependent transcription but conversely down-regulated Hath1-mediated, E-box–dependent transcription in 293T cells.

SW480 cells. For this purpose, Myc-tagged ubiquitin and Flag-Hath1 were coexpressed in SW480 cells and, subsequently, proteasome-mediated degradation was inhibited by MG132. When the cell lysates were immunoprecipitated by anti-Flag antibody, conjugation of Myc-tagged ubiquitin to Flag-Hath1 protein was detectable by immunoblot using anti-Myc antibody (Figure 2*C*). Ubiquitinated Hath1 protein appeared as a broad band on the membrane, suggesting that it is conjugated with random numbers of multiple ubiquitins (polyubiquitinated). Reprobing the same membrane (Re IB) with anti-FLAG antibody showed efficient immunoprecipitation of FLAG-Hath1 protein only in MG132-treated conditions, because FLAG-Hath1 proteins are readily ubiquitinated and degradated in other conditions (Figure 2*C*). These results collectively suggested that Hath1 proteins are polyubiquitinated before degradation by the proteasome-mediated proteolysis in colon cancer cells.

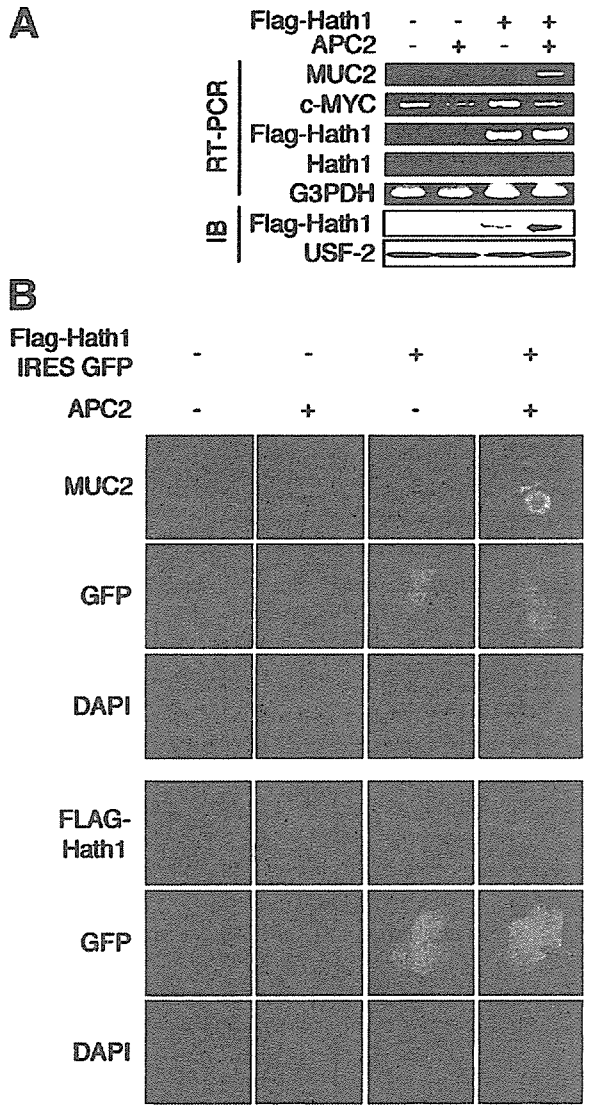

Figure 5. Inactivation of canonical Wnt signaling is required for Hath1-mediated colonocyte differentiation. (*A*) Suppression of canonical Wnt signaling in colon cancer cells is required for Hath1-mediated colonocyte differentiation. Expression plasmids for Flag-Hath1 and APC2 were cotransfected into SW480 cells. Expression of MUC2, C-MYC, Flag-Hath1, endogenous Hath1 (Hath1), and G3PDH mRNA was analyzed by RT-PCR. In the same experiment, protein expression of Flag-Hath1 and USF2 was examined by immunoblotting (IB). The expression of the goblet cell–specific gene *MUC2* was induced only when both FLAG-Hath1 and APC2 were expressed in SW480 cells. (*B*) MUC2 protein is expressed in cells that Hath1 protein stabilized by suppression of Wnt signaling. A bicistronic expression vector pMX-Flag-Hath1-IRES-GFP or its empty control was cotransfected with an expression vector for APC2 into SW480 cells. Cells were stained by fluorescent immunocytochemistry for MUC2 (*upper half, red*) or Flag-Hath1 (*lower half, red*). The green signal of green fluorescent protein (GFP) represents transcription of Flag-Hath1, encoded upstream of GFP and the IRES element. Expression of MUC2 protein is induced only when FLAG-Hath1 protein is stabilized by cotransfecting FLAG-Hath1 and APC2 into SW480 cells. DAPI, 4′,6-diamidino-2-phenylindole.

GSK3β-Mediated Hath1 Proteolysis in Colon Cancer Cells Critically Requires S54 and S58 of Hath1 Protein

Former results confirmed that Hath1 protein is constitutively degradated by proteasome-mediated proteolysis in colon cancer cells. This raised the question whether there is a specific region within the Hath1 protein that is critically required for the present proteolysis system. Although it is well known that Hath1 protein contains a basic helix-loop-helix domain that is critically required for binding to the target sequence of DNA,[26,29] other regions of the protein have not been functionally characterized. To determine the region that may be critically required for the degradation of Hath1 protein, various mutants of Flag-tagged Hath1 protein (Figure 3*A*) were expressed in SW480 cells (Figure 3*B*). Immunoblot using anti-Flag antibody revealed that, although a trace amount of Flag-tagged protein was detected without MG132 treatment by increasing the amount of loaded lysates, deleting up to 53 amino acids of the N-terminal end (N1 to N3), or 140 amino acids of the C-terminal end (C1 and C2), appeared to have no effect on protein stability of the Hath1 protein. However, deletions up to 74 or 109 amino acids of the N-terminal end (N4 and N5) showed markedly stable expression of Hath1 protein without MG132 treatment. These results indicated that the region between amino acids 54 and 74 is critically required for proteasome-mediated Hath1 proteolysis.

The region between amino acids 54 and 74 of the Hath1 protein included 2 serine and 3 threonine residues. It is well known that one of the important mechanisms required for proteasome-dependent degradation is the phosphorylation of specific amino acid residues.[30,31] Based on these data, we searched, using Scansite software (Scansite, Boston, MA), for whether a putative phosphorylation site may exist within the region between amino acids 54 and 74 of the Hath1 protein. Surprisingly, a distinct site extending from serine residue at position 54 (S54) to position 58 (S58) matched the consensus substrate sequence (S/T-X-X-X-S/T) for GSK3β (Figure 3*A*). These results raised a possibility that Hath1 protein is a substrate of GSK3β, and therefore Hath1 protein degradation is regulated by the phosphorylation of specific serine residues by GSK3β. To determine whether kinase activity of GSK3β is required for Hath1 protein degradation, SW480 cells were treated with inhibitors of various protein kinases and examined for FLAG-Hath1 protein expression by immunoblot (Figure 3*C*). Confirming the in silico search for putative phosphorylation sites, FLAG-Hath1 protein was stabilized by the proteasome inhibitor, MG132, and kinase inhibitors specific for GSK3β such as LiCl, kenpaullone, and BIO, but not by other kinase inhibitors such as Ro-31-8220, staurosporine, or UO126, which does not inhibit GSK3β.

To further confirm the involvement of GSK3β in Hath1 proteolysis, we used an siRNA-mediated gene knockdown system to specifically knock down GSK3β gene expression in colon cancer cells. Transfection of GSK3β-specific siRNA into SW480 cells successfully decreased both mRNA and protein expression of GSK3β in SW480 cells (Figure 3*D*). Under this condition, expression of the cotransfected Flag-Hath1 protein was significantly increased up to a comparable level with MG132 treatment. No change was observed in the quantity of Flag-Hath1 mRNA, suggesting that the increase of Flag-Hath1 protein is due to increased protein stability. These results further confirmed that kinase activity of GSK3β is critically required for Hath1 protein degradation in colon cancer cells.

We next examined whether the 2 serine residues found in the putative GSK3β target region (S54 and S58) are critically required for GSK3β-mediated Hath1 proteolysis. For this purpose, a mutant Flag-Hath1 in which 2 serine residues (S54 and S58) were replaced into 2 alanines (54/58SA) was expressed in SW480 cells. Consistently, examination of protein expression by immunoblot revealed that the 54/58 SA mutant of Hath1 (54/58SA), but not the wild type, showed stable protein expression without inhibition of GSK3β by BIO treatment.

These data collectively indicated that the kinase activity of GSK3β is critically required for the degradation of Hath1 in colon cancer cells and also that the 54th and 58th serine residues of the Hath1 protein are critically required for GSK3β-mediated Hath1 proteolysis.

The Canonical Wnt Pathway Reciprocally Regulates Hath1 and β-catenin Protein Stability and Downstream Transcription Activities via GSK3β

Former findings raised an important question as to how the kinase function of GSK3β for Hath1 proteolysis is regulated by the upstream signaling events in colon cancer cells. GSK3β is known to participate not only in the canonical Wnt pathway but also in other pathways such as insulin signaling.[32] However, it is also known that the kinase activity of GSK3β is regulated by a single signaling pathway within a single cell and is usually not modified or affected by multiple pathways.[33] In most human colorectal cancer cells, Wnt signal is aberrantly activated by various gene mutations. Indeed, all the colon cancer cell lines used in this study harbor mutations in the *APC* gene, which suppress the kinase activity of GSK3β on β-catenin phosphorylation and consequently stabilize β-catenin protein.[18] Moreover, a recent study showed that the Wnt signal activates GSK3 to phosphorylate LRP6 in opposite relationship to β-catenin.[34] Therefore, we hypothesized that GSK3β kinase activity is dominantly regulated by Wnt signaling in colon cancer cells, and the aberrant activation of this signal may be involved in Hath1 protein degradation via GSK3β. To confirm the hypothesis, we first examined whether Hath1 protein may be stabilized by the inactivation of the aberrant Wnt signaling in colon cancer cells. For this purpose, we used SW480 cells, in which aberrant Wnt signaling is caused by truncated mutation of *APC*. When the aberrant Wnt signaling of SW480 cells was

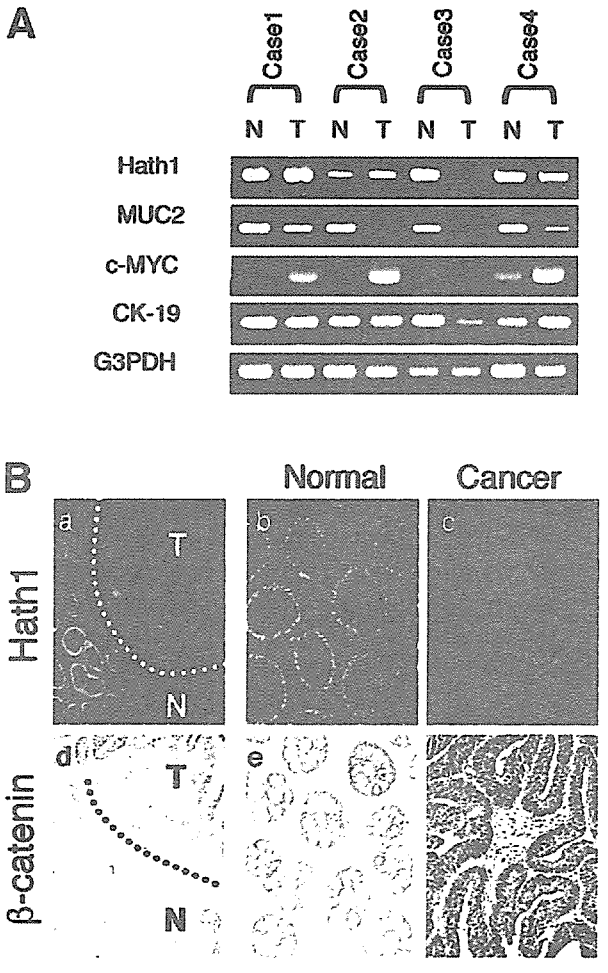

Figure 6. Hath1 protein expression is decreased in human colon cancer tissues expressing Hath1 mRNA and nuclear-located β-catenin protein. (*A*) Hath1 mRNA is expressed in both normal and cancer tissues of human colon. Four cases of colorectal cancer were examined (cases 1–4). N, normal colon mucosa; T, colon cancer tissue of each patient. Semiquantitative analysis of Hath1, C-MYC, MUC2, CK-19, and G3PDH mRNA expression was performed by RT-PCR. CK-19 served as a control for epithelial cell population, whereas G3PDH served as a loading control. In cases 1, 2, and 4, Hath1 mRNA is expressed in both normal and cancer tissue. (*B*) Hath1 protein expression is decreased in colon cancer tissue. The border lesion of the tumor in case 2 was subjected to immunohistochemical analysis. A lower magnification of the border lesion of the tumor (*a* and *d*) and also the magnified view of the cancer tissue (*c* and *f*) and the adjacent normal mucosa (*b* and *e*) are presented. Tissue sections were stained with either anti-Hath1 (Alexa 488, green signal, *a–c*) or anti–β-catenin (diaminobenzidine, brown signal, *d–f*). The figures show a significant decrease of Hath1 staining in cancer tissues compared with normal colonic mucosa, whereas nuclear located β-catenin is significantly increased in cancer tissues (original magnification: *a* and *d*, 100×; *b*, *c*, *e*, and *f*, 400×).

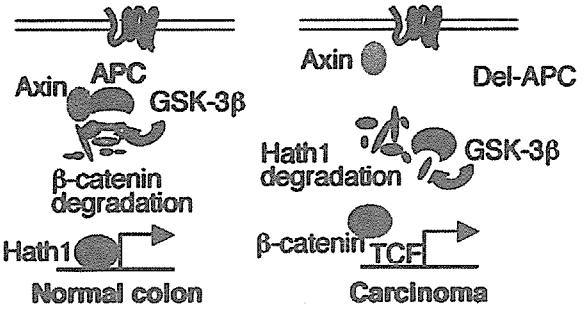

Figure 7. Schematic representation of Wnt-GSK3β–mediated regulation of colonocyte differentiation and proliferation. In normal colonocytes, differentiation is accelerated by turning off the Wnt signaling, which leads to GSK3β-mediated degradation of β-catenin protein and up-regulation of Hath1-mediated transcription of yet-unknown target genes. Conversely, during transformation of colonocytes into carcinoma cells, proliferation is accelerated by constitutive activation of Wnt signaling, which leads to GSK3β-mediated degradation of Hath1 protein and up-regulation of β-catenin/TCF–mediated transcription.

inactivated by transfecting APC mutants (APC2 and APC25) that are capable of forming complexes with β-catenin, Axin, and GSK3β,[22] the amount of endogenous dephosphorylated β-catenin as a stabilized form of β-catenin was significantly decreased but, surprisingly, the expression of cotransfected Flag-WT-Hath1 protein was significantly increased (Figure 4*A*). Transfection of the C-terminal fragment of human APC (APC3; amino acids 2130–2843) that is incapable of forming complexes with β-catenin, Axin, and GSK3β[22] into SW480 cells had no effect on both β-catenin phosphorylation and Flag-Hath1 protein stability (Figure 4*A*). This reciprocal regulation of Hath1 and β-catenin protein stability by Wnt signaling was also observed in 293T cells, in which Wnt signaling is usually inactivated. Activation of Wnt signaling in 293T cells by overexpression of the *Wnt1* gene resulted in a significant increase of the endogenous dephosphorylated, stabilized form of β-catenin protein and also a significant decrease in Flag-Hath1 protein expression. Treatment with MG132 or BIO completely restored the reduction of Flag-Hath1 protein expression induced by activation of Wnt signaling in 293T cells, suggesting that proteasome-mediated Hath1 proteolysis is regulated by the kinase activity of GSK-3β downstream of the canonical Wnt pathway (Figure 4*B*).

We further examined whether Wnt-GSK3β–mediated reciprocal regulation of Hath1 and β-catenin protein stability may also change the transcriptional activity of the corresponding downstream target genes of each protein. Consistent with previous reports,[22] expression of APC2 in SW480 cells decreased the ratio of TOPflash and FOPflash reporter activity by 0.14-fold, regardless of Flag-Hath1 cotransfection (Figure 4*C*). In sharp contrast, E-box–dependent reporter activity was increased by 2.3-fold by cotransfection of APC2 with Flag-Hath1 compared with single transfection of Flag-Hath1 into SW480 cells (Figure 4*C*). Thus, expression of APC2 in SW480 cells significantly down-regulated β-catenin/TCF–dependent transcription but conversely up-regulated Hath1-mediated, E-box–dependent transcription. In contrast, forced expression of *Wnt1* gene in 293T cells up-regulated the ratio of TOPflash and FOPflash reporter activity by 6-fold and, conversely, when Wnt1 was coexpressed with Flag-Hath1 in 293T cells, E-box–dependent reporter activity was down-regulated by 0.6-fold (Figure 4*D*). Thus, expression of Wnt1 in 293T cells significantly up-regulated β-catenin/TCF–dependent transcription but conversely down-regulated Hath1-mediated, E-box–dependent transcription. Single transfection of APC2 or Wnt1 does not change E-box–dependent transcription activity in both SW480 and 293T cells, suggesting that the observed E-box–dependent transcriptional activity represents Hath1-mediated transcription.

These data collectively indicated that GSK3β-mediated proteolysis of Hath1 protein observed in colon cancer cells is dependent on the aberrant activation of the canonical Wnt pathway and that GSK3β reciprocally regulates Hath1 and β-catenin protein stability in a Wnt-dependent manner, directly leading to significant changes in transcriptional activity of the downstream target genes.

Inactivation of Canonical Wnt Signaling Is Required for Hath1-Mediated Colonocyte Differentiation

It is well known that β-catenin/TCF–dependent transcription often promotes cell proliferation, whereas Hath1-dependent transcription promotes cell differentiation. Therefore, we next examined whether the Wnt-GSK3–mediated, reciprocal regulation of β-catenin and Hath1 protein stability and function may regulate the differentiation of colonocytes. For this purpose, we examined whether stabilization of Hath1 protein induced by inactivation of Wnt signaling may lead to spontaneous differentiation of poorly differentiated colon cancer cells. Consistent with former results, single transfection of APC2 into SW480 cells down-regulated mRNA expression of c-Myc but had no effect on colonocyte differentiation (Figure 5*A*). However, when Flag-Hath1 was cotransfected with APC2 in SW480 cells, Hath1 protein was stably expressed and subsequently induced expression of MUC2 mRNA, a specific marker for goblet cell differentiation.[35,36] Immunocytochemical analysis of Hath1 and MUC2 protein expression in SW480 cells showed that both stabilization of Flag-Hath1 protein and up-regulation of MUC2 protein expression were induced under the same condition (Figure 5*B*). Moreover, MUC2 protein was detected exclusively in green fluorescent protein–positive cells that were the bicistronic expression of *Flag-Hath1* gene, indicating that Hath1 protein caused the increase of MUC2 protein (Figure 5*B*).

Collectively, these results suggested that both inactivation of Wnt signaling and stable expression of Hath1

protein are required for colonocyte differentiation toward goblet cells.

A previous report showed that merely inactivating the aberrant Wnt signaling in HT-29 cells induced significant up-regulation of the *MUC2* gene.[19] In our experience, HT-29 cells are different from SW480 cells, because they readily express a small amount of Hath1 and MUC2 mRNA (data not shown). Thus, we speculate that inactivation of aberrant Wnt signaling in HT-29 cells may have up-regulated both mRNA expression and protein stability of the endogenous *Hath1* gene, leading to the significant up-regulation of MUC2 expression.

Hath1 Protein Expression Is Decreased in Human Colon Cancer Tissues Expressing Hath1 mRNA and Nuclear-Located β-catenin Protein

To reveal the role of Wnt-GSK3–mediated reciprocal proteolytic regulation of β-catenin and Hath1 in vivo, we analyzed the correlation between Hath1 mRNA, Hath1 protein, and nuclear localized β-catenin protein expression in human colon cancer tissues. In 3 of 4 cases, we found that tumor tissues expressed Hath1 mRNA at an amount comparable to the adjacent normal mucosa, as judged by RT-PCR (Figure 6*A*). Constitutive activation of Wnt signaling in cancer tissue of these cases was confirmed by the significant expression of *c-MYC*, one of the well-known target genes by β-catenin/TCF. Strikingly, in these cases, immunohistochemical analysis revealed that Hath1 protein is expressed in the normal mucosa but not in the tumor lesion (Figure 6*B*). In contrast, nuclear localized β-catenin protein was easily observed in the tumor lesion but was hardly found in the normal mucosa (Figure 6*B*). These data indicated that at least in some populations of colon cancers, Hath1 expression might be strictly suppressed by Wnt-mediated protein degradation, rather than the suppression of mRNA expression, thereby contributing to maintenance of the undifferentiated state of the tumor tissue.

Discussion

The present study describes a novel function of the canonical Wnt signaling, reciprocally regulating Hath1 and β-catenin protein stability via GSK3β (Figure 7). The "on" and "off" status of the Wnt signal directly converted the target of GSK3β between Hath1 and β-catenin protein, leading to subsequent protein degradation. Our results suggest that this mechanism not only regulates the amount of Hath1 and β-catenin protein expression but also contributes to the significant change in the expression of the downstream target genes and to the cell fate decision between cell differentiation and proliferation. Furthermore, our observations that the dysregulation of the Wnt pathway by components upstream of GSK3β, such as APC, not only contribute to the activation of β-catenin/TCF transcription but also induce concomitant destruction of the gut-specific transcription factor Hath1, provides new insights into the tissue-specific processes of colon cancer development.

It is known that the ubiquitin-proteasome pathway plays crucial roles in the carcinogenesis of some tissues by regulating the protein expression of transcriptional factors such as nuclear factor κB[37] and hypoxia-inducible factor 1.[38] However, our findings suggest that proteolytic regulation of Hath1 protein expression by the ubiquitin-proteasome pathway is a tissue-specific event observed exclusively in colon cancer cells. Moreover, the present system has an outstanding advantage for colon cancer carcinogenesis, in that a single mutation of an upstream gene in Wnt signaling could accelerate cell proliferation by β-catenin/TCF–dependent transcription and immediately shut down cell differentiation at the same time by rapid degradation of Hath1 protein, regardless of Hath1 mRNA expression. Therefore, the present function of the Wnt-GSK pathway further emphasizes the importance of aberrant Wnt signaling in colonocyte transformation.

This study also provides a new insight into the canonical Wnt pathway, because it indicates that GSK3β functions continuously, even when the upstream signal is inactivated, by changing its substrate specificity according to the upstream signal status. It is known that GSK3β changes target amino acid residue within a single substrate protein such as Map1b[39] and Snail,[40] depending on its upstream signals. Our study suggests for the first time that GSK3β could even change the substrate protein itself due to upstream Wnt signaling, leading to immediate degradation of the substrate protein by the ubiquitin-proteasome system. However, the present study could not provide precise evidence to understand whether Hath1 is directly phosphorylated by GSK3β or how changes of GSK3β target are sequentially regulated between Hath1 and β-catenin. In our recent study, in vitro kinase assay using recombinant Hath1 protein and activated GSK3β did not show any phosphorylation of Hath1 protein (data not shown). This result indicated that the phosphorylation of Hath1 might require specific adapter proteins such as Axin and APC to form a complex with GSK3β, as is the case with phosphorylation of β-catenin. However, so far we cannot completely exclude that the effect of GSK3β activity on Hath1 protein stability is possibly indirect. Overexpression of GSK3β had no effect on Hath1 and β-catenin protein stability, suggesting that the total amount of GSK3β protein is abundant enough and does not contribute to limit the substrate protein (data not shown). Thus, it is more likely that Wnt signal controls target specificity of the GSK3β by regulating the complex formation of the substrate with GSK3β and a yet-unknown adapter protein.

In summary, we showed for the first time a novel function of the Wnt-GSK3 signaling pathway, working as a molecular switch changing the cell fate between differentiation and proliferation by proteolytic, reciprocal reg-

ulation of Hath1 and β-catenin in colonocytes. Moreover, the aberrant Wnt signaling contributes to the carcinogenesis of colon cancers not only by the stabilization of β-catenin protein but also by the degradation of Hath1 protein in an intestine-specific manner. These findings provide better understanding of the molecular mechanism regulating Wnt-mediated carcinogenesis in colorectal cancers and further emphasize the importance of aberrant Wnt signaling in colonocyte transformation.

References

1. Booth C, Brady G, Potten CS. Crowd control in the crypt. Nat Med 2002;8:1360–1361.
2. El-Assal ON, Besner GE. HB-EGF enhances restitution after intestinal ischemia/reperfusion via PI3K/Akt and MEK/ERK1/2 activation. Gastroenterology 2005;129:609–625.
3. Haramis AP, Begthel H, van den Born M, van Es J, Jonkheer S, Offerhaus GJ, Clevers H. De novo crypt formation and juvenile polyposis on BMP inhibition in mouse intestine. Science 2004; 303:1684–1686.
4. Cheng H, Leblond CP. Origin, differentiation and renewal of the four main epithelial cell types in the mouse small intestine. V. Unitarian theory of the origin of the four epithelial cell types. Am J Anat 1974;141:537–561.
5. Gowan K, Helms AW, Hunsaker TL, Collisson T, Ebert PJ, Odom R, Johnson JE. Crossinhibitory activities of Ngn1 and Math1 allow specification of distinct dorsal interneurons. Neuron 2001;31: 219–232.
6. Ben-Arie N, Bellen HJ, Armstrong DL, McCall AE, Gordadze PR, Guo Q, Matzuk MM, Zoghbi HY. Math1 is essential for genesis of cerebellar granule neurons. Nature 1997;390:169–172.
7. Leonard JH, Cook AL, Van Gele M, Boyle GM, Inglis KJ, Speleman F, Sturm RA. Proneural and proneuroendocrine transcription factor expression in cutaneous mechanoreceptor (Merkel) cells and Merkel cell carcinoma. Int J Cancer 2002;101:103–110.
8. Bermingham NA, Hassan BA, Price SD, Vollrath MA, Ben-Arie N, Eatock RA, Bellen HJ, Lysakowski A, Zoghbi HY. Math1: an essential gene for the generation of inner ear hair cells. Science 1999;284:1837–1841.
9. Yang Q, Bermingham NA, Finegold MJ, Zoghbi HY. Requirement of Math1 for secretory cell lineage commitment in the mouse intestine. Science 2001;294:2155–2158.
10. Fre S, Huyghe M, Mourikis P, Robine S, Louvard D, Artavanis-Tsakonas S. Notch signals control the fate of immature progenitor cells in the intestine. Nature 2005;435:964–968.
11. Jensen J, Pedersen EE, Galante P, Hald J, Heller RS, Ishibashi M, Kageyama R, Guillemot F, Serup P, Madsen OD. Control of endodermal endocrine development by Hes-1. Nat Genet 2000; 24:36–44.
12. Sekine A, Akiyama Y, Yanagihara K, Yuasa Y. Hath1 up-regulates gastric mucin gene expression in gastric cells. Biochem Biophys Res Commun 2006;344:1166–1171.
13. Batlle E, Henderson JT, Beghtel H, van den Born MM, Sancho E, Huls G, Meeldijk J, Robertson J, van de Wetering M, Pawson T, Clevers H. Beta-catenin and TCF mediate cell positioning in the intestinal epithelium by controlling the expression of EphB/ephrinB. Cell 2002;111:251–263.
14. Huelsken J, Behrens J. The Wnt signalling pathway. J Cell Sci 2002;115:3977–3978.
15. Polakis P. Wnt signaling and cancer. Genes Dev 2000;14:1837–1851.
16. Marshman E, Booth C, Potten CS. The intestinal epithelial stem cell. Bioessays 2002;24:91–98.
17. Pinto D, Gregorieff A, Begthel H, Clevers H. Canonical Wnt signals are essential for homeostasis of the intestinal epithelium. Genes Dev 2003;17:1709–1713.
18. Polakis P. The oncogenic activation of beta-catenin. Curr Opin Genet Dev 1999;9:15–21.
19. Leow CC, Romero MS, Ross S, Polakis P, Gao WQ. Hath1, down-regulated in colon adenocarcinomas, inhibits proliferation and tumorigenesis of colon cancer cells. Cancer Res 2004;64: 6050–6057.
20. Shimura H, Hattori N, Kubo S, Mizuno Y, Asakawa S, Minoshima S, Shimizu N, Iwai K, Chiba T, Tanaka K, Suzuki T. Familial Parkinson disease gene product, parkin, is a ubiquitin-protein ligase. Nat Genet 2000;25:302–305.
21. Onishi M, Kinoshita S, Morikawa Y, Shibuya A, Phillips J, Lanier LL, Gorman DM, Nolan GP, Miyajima A, Kitamura T. Applications of retrovirus-mediated expression cloning. Exp Hematol 1996; 24:324–329.
22. Munemitsu S, Albert I, Souza B, Rubinfeld B, Polakis P. Regulation of intracellular beta-catenin levels by the adenomatous polyposis coli (APC) tumor-suppressor protein. Proc Natl Acad Sci U S A 1995;92:3046–3050.
23. Nishita M, Hashimoto MK, Ogata S, Laurent MN, Ueno N, Shibuya H, Cho KW. Interaction between Wnt and TGF-beta signalling pathways during formation of Spemann's organizer. Nature 2000;403:781–785.
24. Oshima S, Nakamura T, Namiki S, Okada E, Tsuchiya K, Okamoto R, Yamazaki M, Yokota T, Aida M, Yamaguchi Y, Kanai T, Handa H, Watanabe M. Interferon regulatory factor 1 (IRF-1) and IRF-2 distinctively up-regulate gene expression and production of interleukin-7 in human intestinal epithelial cells. Mol Cell Biol 2004; 24:6298–6310.
25. Matsumoto T, Okamoto R, Yajima T, Mori T, Okamoto S, Ikeda Y, Mukai M, Yamazaki M, Oshima S, Tsuchiya K, Nakamura T, Kanai T, Okano H, Inazawa J, Hibi T, Watanabe M. Increase of bone marrow-derived secretory lineage epithelial cells during regeneration in the human intestine. Gastroenterology 2005;128:1851–1867.
26. Akazawa C, Ishibashi M, Shimizu C, Nakanishi S, Kageyama R. A mammalian helix-loop-helix factor structurally related to the product of Drosophila proneural gene atonal is a positive transcriptional regulator expressed in the developing nervous system. J Biol Chem 1995;270:8730–8738.
27. Ciechanover A. The ubiquitin-proteasome proteolytic pathway. Cell 1994;79:13–21.
28. Hochstrasser M. Ubiquitin-dependent protein degradation. Annu Rev Genet 1996;30:405–439.
29. Massari ME, Murre C. Helix-loop-helix proteins: regulators of transcription in eucaryotic organisms. Mol Cell Biol 2000;20: 429–440.
30. Roos-Mattjus P, Sistonen L. The ubiquitin-proteasome pathway. Ann Med 2004;36:285–295.
31. Weissman AM. Themes and variations on ubiquitylation. Nat Rev Mol Cell Biol 2001;2:169–178.
32. Cross DA, Alessi DR, Cohen P, Andjelkovich M, Hemmings BA. Inhibition of glycogen synthase kinase-3 by insulin mediated by protein kinase B. Nature 1995;378:785–789.
33. Doble BW, Woodgett JR. GSK-3: tricks of the trade for a multitasking kinase. J Cell Sci 2003;116:1175–1186.
34. Zeng X, Tamai K, Doble B, Li S, Huang H, Habas R, Okamura H, Woodgett J, He X. A dual-kinase mechanism for Wnt co-receptor phosphorylation and activation. Nature 2005;438:873–877.
35. Chang SK, Dohrman AF, Basbaum CB, Ho SB, Tsuda T, Toribara NW, Gum JR, Kim YS. Localization of mucin (MUC2 and MUC3) messenger RNA and peptide expression in human normal intestine and colon cancer. Gastroenterology 1994;107:28–36.
36. Katz JP, Perreault N, Goldstein BG, Lee CS, Labosky PA, Yang VW, Kaestner KH. The zinc-finger transcription factor Klf4 is

required for terminal differentiation of goblet cells in the colon. Development 2002;129:2619–2628.
37. Greten FR, Eckmann L, Greten TF, Park JM, Li ZW, Egan LJ, Kagnoff MF, Karin M. IKK beta links inflammation and tumorigenesis in a mouse model of colitis-associated cancer. Cell 2004; 118:285–296.
38. Koshiji M, Kageyama Y, Pete EA, Horikawa I, Barrett JC, Huang LE. HIF-1 alpha induces cell cycle arrest by functionally counteracting Myc. EMBO J 2004;23:1949–1956.
39. Trivedi N, Marsh P, Goold RG, Wood-Kaczmar A, Gordon-Weeks PR. Glycogen synthase kinase-3 beta phosphorylation of MAP1B at Ser1260 and Thr1265 is spatially restricted to growing axons. J Cell Sci 2005;118:993–1005.
40. Zhou BP, Deng J, Xia W, Xu J, Li YM, Gunduz M, Hung MC. Dual regulation of Snail by GSK-3beta-mediated phosphorylation in control of epithelial-mesenchymal transition. Nat Cell Biol 2004; 6:931–940.

Received May 17, 2006. Accepted October 5, 2006.

Address requests for reprints to: Mamoru Watanabe, MD, PhD, Department of Gastroenterology and Hepatology, Graduate School, Tokyo Medical and Dental University, 1-5-45, Yushima, Bunkyo-ku, Tokyo 113-8519, Japan. e-mail: mamoru.gast@tmd.ac.jp.

Supported in part by grants-in-aid for Scientific Research, Scientific Research on Priority Areas, Exploratory Research, and Creative Scientific Research from the Japanese Ministry of Education, Culture, Sports, Science and Technology; the Japanese Ministry of Health, Labor and Welfare; the Japan Medical Association; the Foundation for Advancement of International Science; Terumo Life Science Foundation; Ohyama Health Foundation; Yakult Bio-Science Foundation; and the Research Fund of Mitsukoshi Health and Welfare Foundation.

The authors thank Dr Akira Kikuchi (Hiroshima University), Dr Hiroshi Shibuya (Tokyo Medical and Dental University), and Dr Keiji Tanaka (Tokyo Metropolitan Institute) for technical advice.

doi:10.1111/j.1440-1746.2006.04391.x

GASTROENTEROLOGY

Ameliorating effect of saporin-conjugated anti-CD11b monoclonal antibody in a murine T-cell-mediated chronic colitis

Takanori Kanai,* Koji Uraushihara,* Teruji Totsuka,* Yasuhiro Nemoto,* Rei Fujii,* Takahiro Kawamura,* Shin Makita,* Daisuke Sawada,* Hideo Yagita,† Ko Okumura† and Mamoru Watanabe*

*Department of Gastroenterology and Hepatology, Graduate School of Medicine, Tokyo Medical and Dental University and †Department of Immunology, Juntendo University School of Medicine, Tokyo, Japan

Key words
Crohn's disease, macrophages, murine model, targeting, therapy.

Accepted for publication 7 April 2005.

Correspondence
Dr Takanori Kanai, Department of Gastroenterology and Hepatology, Graduate School, Tokyo Medical and Dental University, 1-5-45 Yushima, Bunkyo-ku, Tokyo 113-8519, Japan. Email: taka.gast@tmd.ac.jp

Abstract

Background: Crohn's disease (CD) is an inflammatory bowel disease that is associated with several changes in the immune system, including an increased number of infiltrating macrophages. These macrophages release a variety of pro-inflammatory cytokines, such as tumor necrosis factor-α (TNF-α) which are critically involved in the onset and the development of CD. The present study was performed to explore the initial involvement of macrophages in the development of T-cell-mediated chronic colitis.

Methods: The effects were evaluated of saporin-conjugated anti-CD11b monoclonal antibody (mAb) on the development of chronic colitis in severe combined immunodeficiency (SCID) mice induced by adoptive transfer of $CD4^+CD45RB^{high}$ T cells as an animal model of CD.

Results: Significantly increased CD11b-expressing macrophages as well as $CD4^+$ T cells were found in inflamed colon from colitic mice. Administration of saporin-conjugated anti-CD11b mAb markedly ameliorated the clinical and histopathological disease. *In vivo* treatment with saporin-conjugated anti-CD11b mAb decreased $CD4^+$ T-cell infiltration in the colon and suppressed inferferon-γ (IFN-γ) and TNF-α production by lamina propria $CD4^+$ T cells.

Conclusions: Collectively, the present results suggest an initial role of macrophages in the pathogenesis of T-cell-mediated chronic colitis. Furthermore, the macrophage-specific targeting may be a promising strategy for therapeutic intervention in CD.

Introduction

Crohn's disease (CD) is a chronic inflammatory bowel disease (IBD) characterized by massive infiltration of macrophages and $CD4^+$ T cells in the colon and the small intestine. Although its etiology remains unclear, it has been established that pro-inflammatory cytokines, such as tumor necrosis factor-α (TNF-α), interleukin (IL)-6, IL-12, IL-18 and macrophage infiltrating factor (MIF), produced by macrophages play a pivotal role in the pathogenesis of CD.[1–3] During the inflammatory process of CD, these cytokines are increasingly secreted by macrophages. In addition, macrophages have the capacity to present antigens and to stimulate T cells of the specific immune system, although this antigen-presenting function may be mainly ascribed to dendritic cells (DC) in the gut.[4,5] It has been shown that, in human colon, macrophages are concentrated in a band immediately beneath the luminal epithelium.[6] Thus, macrophages might normally serve as a first line of defense by non-specifically eliminating particles or organisms that have penetrated the intestinal lumen. Furthermore, mucosal macrophages bearing surface markers indicating the presence of an increased activation state are more marked within inflamed mucosa from CD.[7] This increased state of activation is associated with increased functional activity and increased production of pro-inflammatory mediators, and is obviously furthered by an inadequate inflammatory response.[7,8]

To assess the role of macrophages in the development of colitis, we recently investigated the model of 2,4,6-trinitrobenzene sulfonic acid (TNBS)-induced colitis and focused in particular on the role of IL-18 produced by macrophages.[9] It is hypothesized that the ethanol used as a vehicle in the rectal administration of TNBS disrupts the mucosal epithelial barrier, enabling this hapten to bind covalently to protein of colonic epithelial cells and modify cell-surface proteins. Fragments of these altered cells can be taken up by macrophages and DC for presentation to T cells as antigens, resulting in the development of a T-helper 1 (Th1)-dominated colitis. In fact, administration of an antibody conjugated to the

Journal of Gastroenterology and Hepatology 21 (2006) 1136–1142

ribosome-inactivating protein saporin and directed against CD11b-expressing macrophages resulted in protection against TNBS-induced colitis. These results clearly demonstrate a crucial role of infiltrating macrophages in the initial pathogenesis of experimental colitis induced by the hapten TNBS.

To extend the aforementioned hypothesis, we here investigate the initial role of CD11b-expressing macrophages in the development of another T-cell-mediated chronic colitis model, which is induced by adoptive transfer of $CD4^+CD45RB^{high}$ T cells to severe combined immunodeficiency (SCID) mice.[10] In the present study we characterize the ameliorating effects of the ribosome-inactivating protein saporin directed against CD11b-expressing macrophages in preventive settings.

Methods

Animals

Six–8-week-old female C.B.17 scid/scid (SCID) mice and female BALB/c mice were purchased from Japan Clea (Tokyo, Japan) and maintained in a specific pathogen-free condition at Tokyo Medical and Dental University. The Institutional Committee on Animal Research in Tokyo Medical and Dental University approved the experiments.

Induction of colitis and saporin-conjugated anti-CD11b mAb treatment

Colitis was induced in SCID mice by the adoptive transfer of $CD4^+CD45RB^{high}$ T cells, essentially as described previously.[11] In brief, $CD4^+$ T cells were isolated from BALB/c splenic mononuclear cells using the anti-CD4 (L3T4) MACS magnetic separation system (Miltenyi Biotec, Auburn, CA, USA) according to the manufacturer's instructions. Enriched $CD4^+$ T cells were labeled with phycoerythrin (PE)-conjugated antimouse CD4 mAb (RM4-4, BD PharMingen, San Diego, CA, USA) and fluorescein isothiocyanate (FITC)-conjugated anti-CD45RB mAb (16 A, BD PharMingen) and sorted into $CD45RB^{high}$ (highest staining 30%) and $CD45RB^{low}$ (lowest staining 30%) fractions on a FACS-Vantage (Becton Dickinson, Sunnyvale, CA, USA). To assess the effect of saporin-conjugated anti-CD11b mAb (Advanced Targeting Systems, San Diego, CA, USA) in the development of chronic colitis, 12.5 μg anti-Mac-1-saporin in 100 μL phosphate-buffered saline (PBS) was given by i.p. injection 1 and 8 days after T-cell transfer. Control mice received PBS alone or a mixture of free anti-CD11b mAb (10 μg) and saporin (2.5 μg, Advanced Targeting Systems) in doses matching those in the conjugates. All mice were killed 4 weeks after T-cell transfer for histological examination and preparation of lamina propria mononuclear cells (LPMC).

Disease monitoring and clinical scoring

Mice were weighed and monitored for appearance and signs of soft stool and diarrhea weekly.[12] Clinical score was assessed 4 weeks after T-cell transfer as the sum of three parameters: hunching and wasting, 0 or 1; colon thickening, 0–3 (0, none; 1, mild; 2, moderate; 3, extensive); and stool consistency, 0–3 (0, normal beaded stool; 1, soft stool; 2, diarrhea; 3, gross bloody stool).

Histological examination and immunohistochemistry

Tissue samples were fixed in PBS containing 6% neutral-buffered formalin. Paraffin-embedded sections (5 μm) were stained with hematoxylin and eosin. The degree of inflammation (histological score) was determined as previously described.[12] Tissue samples for immunohistochemistry were embedded in octamer-binding factor (OCT) compound and snap-frozen in liquid nitrogen. Six-μm sections were incubated with biotinylated antimouse CD11b mAb (M1/70; BD Pharmingen) or biotinylated isotype-matched control IgG (BD Pharmingen). Biotinylated antibodies were detected using the Vectastain ABC kit (Vector, Burlingame, CA, USA). The sections were then counterstained with hematoxylin.

Preparation of lamina propria mononuclear cells and splenocytes

For the isolation of LPMC from the colon,[13] the entire length of the intestine was opened longitudinally, washed with PBS, and cut into small pieces. The dissected mucosa was incubated twice with Ca^{2+} Mg^{2+}-free Hanks' balanced salt solution containing 1 mmol/L dithiothreitol (Sigma-Aldrich, St Louis, MO, USA) for 30 min each to remove mucus. The supernatants containing intraepithelial cells and epithelial cells were removed. Collected tissues were treated with 2 mg/mL collagenase A (Worthington Biomedical, Freehold, NJ, USA) and 0.01% DNase (Worthington) in RPMI1640 medium for 2 h. The cells were pelleted twice through a 40% isotonic Percoll solution and then further purified by Ficoll-Hypaque density gradient centrifugation (40%/75%; Amersham Biosciences, Uppsala, Sweden). The lamina propria (LP) $CD4^+$ T cells were obtained by positive selection using the anti-CD4 (L3T4) MACS magnetic separation system (Miltenyi Biotec). The cells were >95% $CD4^+$ when analyzed by flow cytometry. Splenic mononuclear cells were obtained from the same animals by mechanical dissociation of the spleen, followed by Ficoll-Hypaque density gradient centrifugation.

Flow cytometry

Isolated LPMC or splenocytes were preincubated with Fcγ receptor-blocking mAb (2.4G2; BD Pharmingen) for 20 min, followed by incubation with FITC-, PE-, or biotin-labeled mAb for 30 min on ice.[14] Biotinylated mAb were detected with PE-streptavidin. All reagents were obtained from BD PharMingen. Two-color flow cytometric analysis was performed on FACScan (Becton Dickinson) equipped with CellQuest software.

Expression of CD11b on splenocytes after saporin-conjugated anti-CD11b mAb treatment *in vivo*

To determine the effect of saporin-conjugated anti-CD11b mAb *in vivo*, we administered 10 μg of saporin-conjugated anti-CD11b mAb in PBS to normal BALB/c mice and normal C.B17 SCID mice. All mice were killed 72 h after the injection, and the expression of CD11b on splenocyte was analyzed by flowcytometry.